MSU Graduate Theses

Summer 2023

Tissue and Sex-Dependent Regulation of Innate Immunity and RNA Editing in Mice

Kelsey R. Kendrick
Missouri State University, Kelsey317@live.missouristate.edu

Follow this and additional works at: https://bearworks.missouristate.edu/theses

Part of the Biology Commons, Immunity Commons, and the Molecular Biology Commons

TISSUE- AND SEX-DEPENDENT REGULATION OF INNATE IMMUNITY AND RNA

EDITING IN MICE

A Master's Thesis

Presented to

The Graduate College of

Missouri State University

In Partial Fulfillment

Of the Requirements for the Degree

Master of Science, Cell and Molecular Biology

By

Kelsey Kendrick

August 2023

TISSUE- AND SEX-DEPENDENT REGULATION OF INNATE IMMUNITY AND RNA EDITING IN MICE

Biomedical Sciences

Missouri State University, August 2023

Master of Science

Kelsey Kendrick

ABSTRACT

Inflammation occurs as a result of insult or infection within the body. Individual cells respond to inflammation by upregulating genes that help mediate the immune response, such as ADAR1. ADAR1 helps regulate the immune response but also catalyzes a process called RNA editing. RNA editing alters the sequence of select mRNAs to alter the encoded proteins. The result is altered function of the encoded protein, which is often beneficial for the cell. Our goal was to determine how inflammation affects the function of ADAR1. Since we know that the effects of inflammation vary between different organs and sexes, we examined ADAR1 function in heart, brain, and muscle in male and female mice after the introduction of LPS, an inflammation-inducing agent. We found that editing in the heart and brain was unaffected. However, RNA editing of FLNB in skeletal muscle was increased by LPS in males but was unaffected in females. Another RNA editing target, FLNA was unaffected by the treatment of LPS, but showed a sex-dependent difference in editing. These results show that the effects of inflammation may selectively affect the function of FLNB in muscle. Furthermore, expression of inflammatory factors ADAR1, TNFα, and MDA5 was induced by LPS, as expected, but TNFα and MDA5 expression was induced more in females. Our work suggests that the impact of sex on inflammatory factors may also indirectly affect the rate of RNA editing of select transcripts in select tissues.

TISSUE- AND SEX-DEPENDENT REGULATION OF INNATE IMMUNITY AND RNA

EDITING IN MICE

By

Kelsey Kendrick

A Master's Thesis
Submitted to the Graduate College
Of Missouri State University
In Partial Fulfillment of the Requirements
For the Degree of Master of Science, Cell and Molecular Biology

August 2023

Approved:

Randi J. Ulbricht, Ph.D., Thesis Committee Chair

Amanda Brodeur, M.D., Ph.D., Committee Member

Amy Hulme, Ph.D., Committee Member

Julie Masterson, Ph.D., Dean of the Graduate College

In the interest of academic freedom and the principle of free speech, approval of this thesis indicates the format is acceptable and meets the academic criteria for the discipline as determined by the faculty that constitute the thesis committee. The content and views expressed in this thesis are those of the student-scholar and are not endorsed by Missouri State University, its Graduate College, or its employees.

ACKNOWLEDGEMENTS

I would like to thank the faculty and staff of the Missouri State University Biomedical Science department. Their instruction, support, and encouragement has proven to be invaluable to me and I owe all that I have accomplished in my academic career over the last six years to them. I want to thank the CASL office and SCG for giving me the opportunity to complete this program as well as providing me with incomparable knowledge and experiences that I would not be able to find anywhere else. I would also like to thank my committee members, Dr. Amanda Brodeur and Dr. Amy Hulme for investing their time, energy, and wisdom into me and my thesis research. I appreciate their willingness to share their thoughts, ideas, experience, and excitement with me throughout this process. Dr. Randi J. Ulbricht, thank you for everything that you have done for me these past few years. You have played many roles in my life now from professor, advisor, advocate, to PI. I can confidently say that joining your lab was one of the best decisions that I have made. I will forever cherish the time, knowledge, support, grace, and laughter that you have shared with me. And finally, thank you to my friends and family that I have had from the beginning and to those that I have gained throughout this journey. Thank you for the unwavering love and support that you have shown me and for sticking with me through it all. To my mom, Stephanie, I love you and thank you the most. You have made me into the person that I am today, and I am so proud to have you as a role model.

TABLE OF CONTENTS

LIST OF TABLES

LIST OF FIGURES

LITERATURE REVIEW

Innate Immunity

Innate immunity is the first line of defense in all multicellular organisms against potential pathogens to avoid infection. It is responsible for the rapid, non-specific response towards foreign bodies. The innate immune system is comprised of both physical barriers, such as skin, mucus membranes, and stomach acid, as well as internal defenses such as inflammation, phagocytic cells, and natural killer (NK) cells. This type of defense begins minutes to hours after the invasion of potential pathogens (Aristizábal and González 2013). Double stranded RNA (dsRNA) is a trigger for the innate immune response. Non-self dsRNA in the cytoplasm is detected by dsRNA sensors retinoic acid-inducible gene I (RIG-I) and melanoma differentiation-associated protein 5 (MDA5), which leads to the activation of cytokines, chemokines, and interferon (IFN) gene expression leading to systemic inflammation (Hur 2019). Interferons induce the transcription of genes that are both pro- and anti-inflammatory in order to maintain and control the innate immune response. Hundreds of interferon stimulated genes (ISGs) have been identified and include all type I, II, and III IFNs. While the method of action for many of these ISGs has yet to be discovered, it is known that ISGs help activate the immune response and suppress infections at all stages (Schoggins 2019).

Sex Differences in Innate Immunity

Males and females have differences in the innate immune response to foreign and self-antigens. These differences are attributed to the differential regulation of the immune response due to sex chromosome genes and sex hormones, such as progesterone, androgen, and estrogen.

The differing immune responses seen between males and females result in differential susceptibility to autoimmune diseases, infections, and vaccination outcomes. For example, females make up 80% of the population that is affected by autoimmune diseases, have at least twice as strong of an immune response to seasonal influenza vaccines, and HIV infected females have 40% less HIV viral RNA in their blood (Klein and Flanagan 2016). Transcriptional analyses have revealed sex differences in the induction of the type I IFN response, where females generally mount a stronger innate immune response compared to males. The expression of TLR-pathway and pro-inflammatory genes such as toll-like receptor-7 (TLR7), myeloid differentiation factor 88 (MyD88), retinoic acid-inducible gene I (RIG-I), interferon regulatory factor 7 (IRF7), interferon beta (IFN-β), Janus kinase 2 (JAK2), signal transducer and activator of transcription 3 (STAT3), nuclear factor-κB (NF-κB), interferon gamma (IFN-γ), and tumor necrosis factor (TNF) have been shown to be higher in females following both virus challenge in adult rats and vaccination in adult humans (Hannah et al. 2008; Klein et al. 2010). Furthermore, cells associated with the innate immune system differ in activity and number between the sexes. Natural killer (NK) cell frequencies are higher in males than in females (Abdullah et al. 2012). Females have exhibited higher neutrophil and macrophage phagocytic activity, and their antigen-presenting cells are more efficient (Spitzer 1999; Weinstein and Segal 1984). One inflammatory pathway associated with the innate immune system that has not been investigated for sex differences is the MDA5/MAVS pathway.

MDA5

RIG-I and MDA5 are key protein sensors of the pathogen-associated molecular patterns (PAMPs) responsible for activating innate immunity. RIG-I and MDA5 specifically sense

dsRNA to induce the expression of type-I interferons (INF1) and other pro-inflammatory cytokines during initial stages of infection. MDA5 is comprised of two N terminal caspase activation and recruitment domains (CARDS), a central helicase domain, and a C terminal domain (CTD). The helicase and CTD are involved in RNA binding. Multiple molecules of MDA5 bind along the length of dsRNA, clustering multiple CARDS domains and allowing the activated RIG-I and MDA5 to interact with the mitochondrial antiviral signaling proteins (MAVS). The activation of MAVS triggers a signaling cascade that leads to the transcriptional induction of the IFN1 genes (Junior et al. 2019). These IFN1 genes then stimulate the production of select anti-inflammatory genes that downregulate the signaling cascade and help regulate the immune system, decreasing unnecessary inflammation.

ADAR1 is Anti-Inflammatory

ADAR1 is an anti-inflammatory gene that regulates MDA5 activity. Studies have shown that the lack of ADAR1 results in the inappropriate activation of MDA5, leading to death. The interferon inducible isoform of ADAR1, ADAR1 p150, has a primary physiological function to disrupt the structure of endogenous dsRNA to prevent MDA5 from sensing it as non-self and activating the innate immune system superfluously (Liddicoat et al. 2015).

ADAR1 p150 binds to the dsRNA and destabilizes the double stranded structure by catalyzing adenine-to-inosine (A-to-I) editing within the dsRNA structure. In A-to-I RNA editing, the C6 amine group on adenosine is deaminated, changing it to inosine (Fig. 1). The base pairing structure of inosine is similar to guanosine, therefore editing adenosines within the dsRNA structure disrupts base pairing. This acts to prevent recognition of this molecule as a dsRNA by MDA5 and RIG-I, downregulating the inflammation cascade and IFN production, thus decreasing the amount of inflammation from the innate immune response (George et al.

2016; Fig. 2). This regulation of inflammation is necessary to prevent unnecessary activation of the innate immune pathway. When ADAR1 p150 function or expression are decreased, autoimmune diseases such as Aicardi-Goutières syndrome (AGS) can result. When ADAR1 p150 or ADAR1 are completely disrupted, the organism does not survive. However, when MDA5 is also eliminated, organisms are born healthy, suggesting that ADAR1 p150 is an essential negative regulator of the MDA5/MAVS RNA sensing pathway and is a key mechanism to prevent autoreactivity (Pestal 2015).

ADAR1 p150's role in downregulating MDA5 and immune activation is important to human health. In the autoimmune disease, psoriasis, lesions are formed due to the activation of adaptive and innate immunity. In psoriatic lesions, A-to-I RNA editing is reduced. This reduced editing also reduces inactivation of MDA5, leading to hyperactive immune activation that eventually leads to lesions (Shallev et al. 2018). While this research was unable to differentiate between which ADAR1 isoform had decreased expression, since MDA5 was not downregulated, it might indicate that the ADAR1 p150 was responsible for deregulation. MDA5 has also been implicated in autoimmune and autoinflammatory diseases such as type 1 diabetes (T1D) and systemic lupus erythematosus (SLE). Regulation of MDA5 by ADAR1 p150 likely plays a role in preventing the occurrence of each of these disorders.

The majority of RNA editing and inflammation research has been conducted on global editing levels, however, dysregulated editing of coding RNA has been linked to SLE. Systemic lupus erythematosus is an autoimmune disorder that is characterized by multisystem microvascular inflammation (Cojocaru et al. 2011). In patients that were affected by SLE, 95% of the recoding events that were sequenced experienced higher levels of A-to-I editing than the control samples. Another study aimed to determine the expression of ADAR1 isoforms and

subsequent effects on A-to-I editing of recoding events in the brain in response to viral infection. While this study did determine an increase in ADAR1 p150 there were no significant changes in site-specific A-to-I editing events (Hood et al. 2014). Further investigation into other tissues as well as potential sex differences is needed.

ADARs (Adenosine Deaminase Acting on RNA)

A-to-I RNA editing is a natural process catalyzed by adenosine deaminase acting on RNA (ADAR) (Bass 2002). There are three ADAR genes in mammals: ADAR1, ADAR2, and ADAR3. The ADARs have a common domain organization that includes two or three copies of a double stranded RNA binding domain (dsRBD) in their N-terminal region followed by a C-terminal adenosine deaminase catalytic domain. The catalytic domain of ADAR3 is inactive, while ADAR1 and ADAR2 encode active deaminases. The dsRBD primary function is to bind to dsRNAs (Banerjee 2014), allowing ADARs to recognize their targets and act on adenosines that occur in and around dsRNA strands (Fig. 3).

ADAR2 protein is expressed in many different tissues but has been found to be most strongly expressed in the nervous system (Tan et al. 2017). ADAR2 contains two dsRBDs and a nuclear localization signal in the N-terminus, thus allowing ADAR2 to localize to the nucleus, where it performs its editing co-transcriptionally (Desterro et al. 2003; Fig. 3). ADAR2 edits many mRNAs, including itself and GluA2, affecting both cellular and organismic physiology (Higuchi et al. 2000; Li et al. 2009). Interestingly, ADAR2 self-editing deactivates ADAR2 by producing an alternative 3' splice site, AI (AI is recognized as AG by the spliceosome), that leads to the inclusion of an extra exonic sequence and a frameshift. This leads to a premature stop codon and complete inactivation of the product (Feng et al. 2006).

ADAR3 is catalytically inactive, even though the arrangement and sequence of the deaminase and dsRBDs are similar to ADAR2. The presence of a lysine (R-domain) and arginine rich N-terminal extension distinguishes ADAR3 from ADAR2. The presence of two dsRBDs allows ADAR3 to bind to dsRNA, like ADAR2 and ADAR1. Unlike ADAR1 and ADAR2, ADAR3 also contains a single stranded RNA (ssRNA) binding domain in the R-domain of its N-terminus (Fig. 3). The affinity for dsRNA appears lower in ADAR3 than in ADAR1 and ADAR2 but it does appear to interact with RNA substrates in a unique way due to containing both the double stranded and single stranded RNA binding domains (Chen et al. 2000). Thus, ADAR3 can compete with ADAR1 and ADAR2 for RNA binding of substrates, inhibiting their RNA editing activities when co-expressed. This was observed when ADAR3 suppressed effective editing of the 5-HT$_{2C}$ receptor by 70-80% (Chen et al. 2000).

Isoforms of ADAR1

The ADAR1 gene produces two isoforms, p110 and p150, from alternative promoters (George et al. 2005). ADAR1 p110 is a 110 kilodalton protein that is constitutively expressed while ADAR1 p150 is a larger, 150 kilodalton protein, that is produced from an interferon inducible promoter (George and Samuel 1999; George et al. 2005). The IFN-stimulated response element (ISRE), found in the promoter region of the ADAR1 p150 isoform is responsible for the IFN induced expression. This ISRE, when stimulated with IFN, leads to the production of an alternative promoter upstream of the ADAR1 p110 promoter leading to the transcription of an mRNA with an AUG start codon upstream, but in frame with, the start codon of the ADAR1 p110 isoform (George and Samuel 1999).

The p150 isoform of ADAR1 has an extended N-terminus, resulting in two copies of a Z-DNA binding domain (ZDBD), whereas ADAR1 p110 contains one (Patterson and Samuel 1995). The ZDBD allows ADAR1 to recognize the left-handed helical variant of DNA but the role in A-to-I editing has not been clearly defined (Fig. 3). One possible function could be to direct ADAR1 to actively transcribing genes since localizing ADAR1 to the site of transcription would allow it to edit the RNA prior to splicing (Barraud and Allain 2012). It has also been shown that the binding of ADAR1 to Z-DNA restricts it from adopting another conformation (Berger et al. 1998). This restriction of conformation could play a role in gene expression since the binding around a promoter results in increased levels of transcription (Oh et al. 2002). A recent study has found that the ZDBD, Zα that is unique to the p150 isoform, allows ADAR1 p150 to bind to Z-RNA in the cytoplasm. This binding is necessary for editing cytoplasmic dsRNA and preventing dysregulation of the immune system (Chiang et al. 2020).

ADAR1 p110 is primarily located in the nucleus where its' primary job is to edit RNA co-transcriptionally. The extended N-terminus of ADAR1 p150 contains a nuclear export signal which allows it to shuttle between the nucleus and cytoplasm (Fig. 3). ADAR1 p150 accumulates in the cytoplasm, where it plays its role in regulating innate immunity (Fritz et al. 2009).

ADAR Targets

There are millions of A-to-I RNA editing sites in humans, but most of these sites are in non-coding regions of the transcriptome (Li et al. 2009). The vast majority of these editing sites occur in *Alu* repeat elements that are transcribed as inverted repeats, making long dsRNA. ADARs target double stranded RNA, therefore all RNA editing sites occur in and around regions of dsRNA. Editing with *Alu* sites is generally high in abundance and indiscriminate, known as hyper-editing (Bass 2002). The deamination of select adenosines within coding regions occurs

within short, imperfect dsRNA. The specific RNA editing that alters coding regions often occurs due to dsRNA structure in the pre-mRNA. Intronic *cis* elements called editing site complimentary sequences (ECSs) are complimentary and base pair with exonic sequences that contain the targeted adenosine(s). Structural imperfections within the dsRNA, such as mismatches, bulges, and/or loops, are thought to be responsible for indicating the specific adenosine to target for editing. *In vitro* studies have shown that ADARs will preferentially target adenosines next to a 5' uridine but an adenosine next to a 5' guanosine is rarely targeted (Polson and Bass 1994). Furthermore, when compared to other adenosines, those that are found in mismatches with cytosines are edited more (Wong et al. 2001).

Selective RNA editing is not a mutation or an accident, but an intentional process that provides the cell and the organism with more diverse protein isoforms. For example, the GluA2 subunit of α-Amino-3-hydroxy-5-methyl-4-isoxazolepropionic acid (AMPA) receptors is altered by specific RNA editing to produce a protein isoform that is essential for life. AMPA receptors (AMPARs) are tetrameric, cation permeable ionotropic glutamate receptors expressed throughout the brain. AMPARs are made up of four subunits, GluA1, GluA2, GluA3, and GluA4 (Chater and Goda 2014). The GluA2 subunit is responsible for determining the ability of calcium to enter the cell through the AMPAR. The presence of this subunit is also important for the stability and trafficking of AMPARs within the synapse (Sans et al. 2003). The GluA2 subunit is subjected to editing by ADAR2 which converts a codon for glutamine (CAA) into a codon for arginine (CGA). This amino acid change allows the AMPAR to go from calcium permeable to calcium impermeable. So, the ability of the GluA2 subunit to regulate calcium permeability of AMPAR depends on RNA editing. The GluA2 subunit is edited at nearly 100% in the brain. In fact, presence of the GluA2 from the unedited RNA contributes to excitotoxic cell loss. This

indicates that the RNA editing of this subunit is necessary for normal brain function (Kawahara et al. 2003). Furthermore, it has been suggested that calcium permeable AMPARs that are a result of downregulated GluA2 RNA editing occur in ischemia, epilepsy, and other various neurological diseases (Gorter et al. 1997), suggesting that maintenance of RNA editing is critical to proper brain function.

A-to-I editing occurs at five distinct positions within the mRNA encoding the serotonin receptor 5-HT$_{2C}$, altering three amino acids in the second intracellular loop (Niswender et al. 2001). The A-to-I editing events of these sites can lead to thirty-two mRNA variants giving way to twenty-four different protein isoforms with distinct functions (Fitzgerald et al. 1999). The 5-HT$_{2C}$ receptor is a G protein-coupled receptor (GPCR) that plays a key role in appetite, mood, endocrine secretions, and motor behavior. The 5-HT$_{2C}$ receptor is the only known member of the superfamily of seven transmembrane domain receptors (7TMRs) to be edited due to it possessing an imperfect inverted repeat at the end of exon 5 and the ECS (Exon Complementary Sequence) in the beginning of intron 5 allowing the formation of dsRNA (Burns et al. 1997; Werry et al. 2008). Editing frequency of the serotonin receptor varies between brain regions, resulting in different amounts of each protein isoform to be expressed in these regions. (Wang et al. 2000).

Filamin A (FLNA) and Filamin B (FLNB) are also mammalian editing targets (Tariq and Jantsch 2012). FLNA and FLNB share a common role in stabilizing the actin cytoskeleton of cells and are both ADAR2 targets for editing. The mRNAs encoding FLNA and FLNB undergo RNA editing that leads to a highly conserved glutamine (CAA) to arginine (CGA) change at identical positions (Czermak et al. 2018). FLNA editing has been shown to be conserved among vertebrates and studies have shown that the substantial amount of editing in human and mouse cardiovascular tissue has FLNA as the prominent substrate (Jain et al. 2018). The highest editing

levels of FLNB have been found in skeletal muscles, cartilage, and bones where the function of

FLNB seems to be the most important (Czermak et al. 2018).

2016).
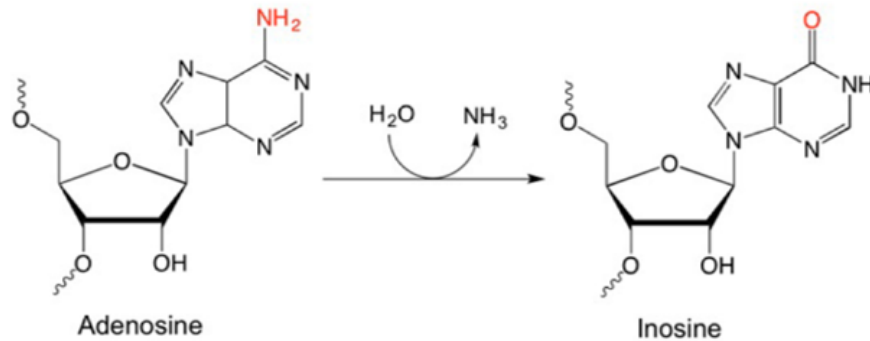
Figure 1. Conversion of Adenosine to Inosine.
The chemical structures of adenosine and inosine are shown. The amine group on adenosine (red) gets converted to oxygen (red) on inosine through hydrolytic deamination (Song et al. 2016).
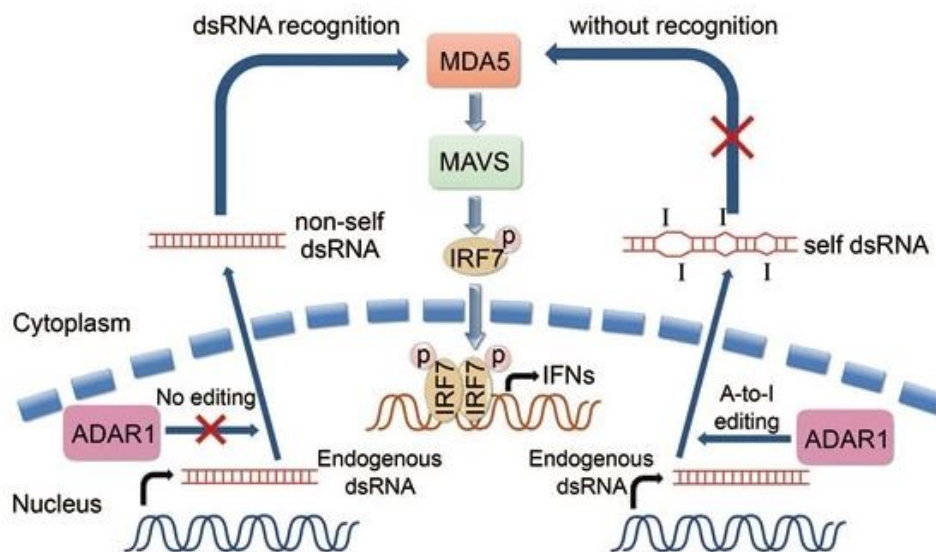
Figure 2. ADAR1 mediated editing of dsRNA.
Double stranded RNA in the cytoplasm is recognized by MDA5 (left), which triggers MAVS activation and then phosphorylation of IRF7. IRF7-P then serves as a transcription factor for activation of IFN inducible genes, including ADAR1 p150. ADAR1 edits cytoplasmic dsRNA preventing recognition by MDA5 and the induction of inflammation. ADAR1 also edited endogenous dsRNA in the nucleus, often co-transcriptionally (Yu et al. 2015).
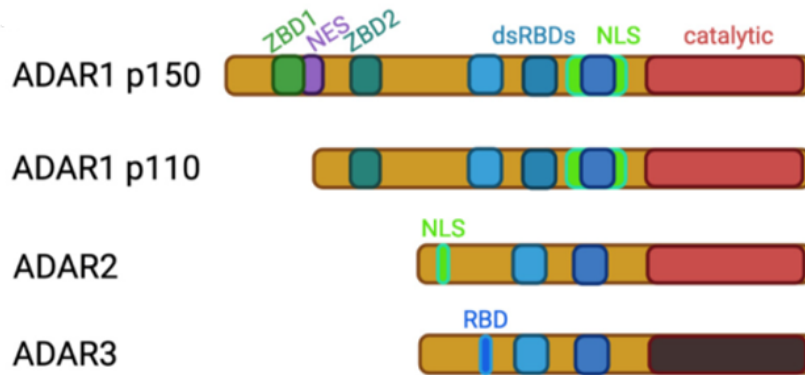
Figure 3. ADAR protein structure.
Three ADAR genes, ADAR1, ADAR2, and ADAR3, can be found in mammals. ADAR1 has two isoforms, the 150 kilodalton (ADAR1 p150) and 110 kilodalton (ADAR1 p110) proteins. All ADARs contain a deaminase domain (catalytic, red), however, ADAR3 is catalytically inactive (black). All ADARs contain double-stranded RNA-binding domains (dsRBDs, light blue) in varying numbers. Both isoforms of ADAR1 contain Z-DNA binding domains (ZDB, green). ADAR1 and ADAR2 contain a nuclear localization signal (NLS, green) and the ADAR1 p150 isoform also contains a nuclear exportation signal (NES, purple). ADAR3 contains an RNA-binding domain (RBD) (Vesely and Jantsch 2021).

Research Goal

Previous research conducted by Claire Nichols aimed to determine if inflammation alters RNA editing in a tissue specific and/or sex-specific manner by investigating RNA levels in the heart, brain, and skeletal muscle during induced inflammation. The editing targets that were investigated included the ADAR2 targets, FLNA and FLNB, and the ADAR1 target CAPS1. Editing was investigated in the heart, brain, and skeletal muscle of both LPS and saline treated mice. The data collected did not show a significant sex-specific difference in the editing of these targets in the heart or brain. However, preliminary data on FLNA in skeletal muscle has shown that editing of this target is reduced by inflammation and that editing in female mice was reduced (in both LPS and saline), compared to males. This data indicates that editing of FLNA in skeletal muscle is sex-dependent, though more data from additional mice is required to validate these findings.

The goal of this thesis research is to confirm this significance and further investigate the sex-dependent differences of inflammation in skeletal muscle. To do this, RNA editing levels of at least 3 targets in inflamed and non-inflamed skeletal muscle tissue will be determined. Inflammation was induced through LPS injections, while control mice were injected with only saline. The tissues were dissected 4 hours after injection. The frozen tissues were stored at -80°C until RNA isolation. The RNA was then subjected to RT-PCR to amplify the region around the editing site and then sequenced by Sanger sequencing or next-generation sequencing (NGS). Claire has isolated RNA and analyzed FLNA editing from three animals in each group. The editing of FLNA from additional animals will be determined, for a final N of at least five (including five LPS-treated males, five LPS-treated females, five saline-treated males, and five saline-treated females). Furthermore, RNA editing levels of FLNB in skeletal muscle of these

same five animals will be quantified to determine if this editing target is also sex-dependent and if inflammation affects editing levels.

ADAR1 has been shown to negatively regulate ADAR2's editing activity (Anantharaman et al. 2017). Due to this competitive inhibition, the editing of ADAR2 targets, along with ADAR1 targets, is likely to be affected by the upregulation of ADAR1 when induced by inflammation. FLNA and FLNB are both ADAR2 targets. To determine if ADAR1 editing is sex-specific and/or affected by inflammation in skeletal muscle an ADAR1 target will be investigated. While Claire's work included analysis of the ADAR1 target CAPS1 in heart and brain, this target is not expressed in skeletal muscle. IGFBP7, BLCAP, and RPA1 are all edited by ADAR1 (Hood et al. 2014; George et al. 2016) and are expressed in skeletal muscle as confirmed using the Mouse Genome Informatics database, thus representing potential RNA for investigation in this study. RNA editing from at least one of these targets will be analyzed from LPS and saline treated skeletal muscle. RT-PCR primers flanking the RNA editing site in the mRNA will be developed using primerBLAST and the primers will be tested on cDNA derived from skeletal muscle. The presence of a robust product, with little background or genomic DNA amplification will indicate an optimal primer set. The PCR product from successful primer sets will be purified and subjected to NGS or Sanger sequencing. For Sanger sequencing, the electropherogram trace must be clear, with minimal background for accurate editing detection. For NGS, there are limits on the size and location of the editing site that may interfere with sequence analysis. Therefore, the target(s) with products (from successful primer sets) and successful sequencing analysis will be chosen for analysis in this thesis.

While Claire's study indicates that inflammation induced changes to RNA editing in skeletal muscle, this tissue has not been analyzed for the amount of ADAR1 p150 induction.

Similarly, the extent of inflammation in this tissue compared to the heart or brain has not been investigated. While LPS is expected to induce systemic inflammation, no differences in editing in the heart and brain may indicate reduced levels of inflammation or ADAR1 induction, compared to the skeletal muscle. Conversely, it is possible that ADAR1 p150 induction is similar, despite the tissue, but that its RNA binding activity (competitive inhibition) and/or RNA editing activity is regulated differently in the muscle. Therefore, the second aim of this research will be to monitor innate immune activation by quantifying ADAR1 p150 levels, as well as a cytokine like TNFα or IL-6 levels in skeletal muscle.

MDA5 levels are known to be higher in females, compared to males (Koeing et al. 2014). Females are also more likely to develop autoimmune diseases. Since ADAR1 p150 is a necessary inhibitor of the MDA5 inflammation pathway, differences seen between sexes and/or tissues could give more insight into the development of autoimmune diseases and the sex-specific difference seen there. To further explore sex-specific and/or tissue specific differences in inflammation, MDA5 levels will be determined by qRT-PCR in heart and skeletal muscle of male and female mice, treated with LPS and saline. ADAR1 p150 levels in heart and skeletal muscle will be compared to these MDA5 levels. If MDA5 levels are sex-dependent, but ADAR1 p150 levels are not, this may suggest that females are more susceptible to autoimmune disease due to reduced control of innate immunity.

METHODS

Injections, Dissections, and RNA Isolation

All mouse manipulation was done by previous graduate students. No live animals were used in this work therefore IACUC approval was not necessary. IBC approval was obtained from Missouri State University (Protocol 2022-04.6 IBC approved 4/28/2022 – 4/27/2024; Appendix A). All necessary CITI certification trainings were completed (Appendix B). Previously, co-housed pairs of mice underwent intraperitoneal injections of either saline (control) or lipopolysaccharide (experimental) once they were between 8 and 13 weeks of age. The lipopolysaccharide (LPS) injections were used to induce acute inflammation in the mice. Four hours after injections the mice were euthanized and then dissected to obtain the brain, right eye, pituitary gland, heart, left kidney, pancreas, and skeletal muscle from the upper left abdominal wall. These tissues were cryopreserved in liquid nitrogen and stored in -80 °C until they were homogenized, and the RNA was isolated. The injections and dissections were performed by former graduate student Christian Rivas. The tissue homogenization and RNA isolation was performed by former graduate student Claire Nichols.

RNA Quantification

To quantify the amount of RNA that was isolated the IMPLEN NanoPhotometer NP80 was used. The RNA was allowed to thaw completely at room temperature. After thawing it was thoroughly vortexed to ensure the RNA was fully resuspended. One microliter of the diethyl pyrocarbonate (DepC) treated water that was used to resuspend the RNA was pipetted onto the nanophotometer and used as the blank. The absorbance was measured in ng/µL and, if accurately blanked, the concentration would read as 0 ng/µL. If the blank was not accurate the process was

redone with the same water until the concentration read 0 ng/µL. The RNA was vortexed again and 1 µL of the RNA sample would be pipetted onto the nanophotometer, and the absorbance was read. The concentration, A_{260}, and A_{260}/A_{280} were recorded. After quantification the RNA samples were either stored at -80 °C or immediately reverse transcribed into cDNA.

Reverse Transcription

The RNA isolated from the homogenized tissues were reverse trasncribed into cDNA. A 20 µL reverse transciption reaction was created using the Applied Biosystems High Capacity cDNA Reverse Transcription Kit (catalog #4368814) with 1 µg of RNA added. Two master mixes were created with the reverse transcription kit. Both master mixes contained the buffer, deoxynucleoside triphosphates (dNTPs), random primers, and water. One master mix contained reverse transcriptase (RT) and the other had water instead of the RT. The master mixes were then aliquoted into PCR tubes. The concentrations of each component of the PCR reactions were 1 X buffer, 0.5 X dNTPs, 1 X random primers, and 1 µL of RT or water. The samples were run in the BIO-RAD T100™ Thermal Cycler under the HC_RT protocol cycling conditions (Table 1). The cDNA made was either stored at 4 °C or immediately used in subsequent experiments.

PCR

Polymerase chain reaction (PCR) was performed on the cDNA to amplify the edited region of the desired target. A master mix containing the forward and reverse primers (Tables 2,3,4), water, and the ThermoScientific 2 X DreamTaq polymerase master mix (catalog #K1081) that contains buffer, dNTPs and Taq polymerase was made. Forty-five microliters of the master mix was aliquoted into PCR tubes. Each PCR reaction contained 400 ng forward primer, 400 ng reverse primer, 25 µL of the DreamTaq green polymerase master mix, and 16 µL of water. Five

microliters of the cDNA was pipetted into the PCR tubes with the master mix to create a 50 µL reaction. Every RT-PCR contained two negative controls, one that contained the no RT cDNA for every sample and one that contained water instead of cDNA. The PCR reactions were then placed in the BIO-RAD T100™ Thermal Cycler and the protocol ran varied based on the proper melting temperature for the intended target.

Agarose Gel Electrophoresis

To verify that the intended target was amplified during PCR, gel electrophroesis was utilized. A 1 %, 1.5 %, or 2 % agarose in 1 X sodium borate (SB) buffer solution was melted in a microwave until the solution was clear throughout. Once this was achieved, 8×10^{-4} mg/mL of ethidium bromide was added to the melted gel solution. This was mixed together and then poured into a gel molding tray. The comb was inserted into the melted gel and the solution was allowed to solidify. After solidification, the comb was removed and the electrophoresis chamber was filled with 1 X SB so that it was covering the solid gel. Five microliters of each PCR product was loaded into each well and 3 µL of the 0.1 µg/µL ThermoScienctific GeneRuler 1kb Plus DNA Ladder (catalog #SM1331) was added to at least one well. The samples were electrophoresed at 250 volts for 20 to 30 minutes. Upon completion of the run the gel was visualized under a UV light on a BioRad GelDoc Go Imaging System (model Ver. A 12012149). The verification of the intended target was determined by the presence of a band at the desired size (Tables 2,3,4) when compared to the ladder in the positive RT samples and no or negligible band in the negative controls.

Purification

After the PCR products were verified, the DNA was gel purified. The remaining PCR product that was not electrophoresed for verification (45 µL) was loaded into one well of an agarose gel. The gel was electrophoresed in the same manner as the verification. Upon completion the gel was viewed using a short wave transilluminator. The bands were cut from the gel using a razor blade. The cut gel slice was carefully placed in a 1.5 mL tube and then weighed. The gel was purified using the Promega Wizard SV Gel and PCR Purification kit (catalog #A9282). An equal amount of the membrane solution as the weight of the band was added to each gel slice (0.430 g = 430 µL of membrane binding solution). The tubes were vortexed and then placed in a 65 °C heating block until the gel was completely melted. The tubes were vortexed and 750 µL of the melted gel was added to a labeled spin column. The spin column was centrifuged at 13,000 x g for 1 minute. The remaining melted gel was added to the spin column, and it was centrifuged at 13,000 x g for 1 minute. The flow through was discarded. Seven hundred microliters of the membrane wash solution were added to the spin column and centrifuged again at 13,000 x g for 1 minute. The flow through was discarded. Then, 500 µL of the membrane wash solution was added to the spin column and centrifuged at 13,000 x g for 1 minute. The flow through was discarded. The spin column was centrifuged again for 5 minutes. The spin column was moved to a new 1.5 mL tube and 30 µL of heated nuclease free water was added and incubated at room temperature for 1 minute. The tubes were then centrifuged at 13,000 x g for 1 minute. A nanophotometer was used to quantify the DNA and the samples were stored at -20 °C.

Sequencing

To determine the amount of editing for each target, purified amplicons were sent to GeneWiz (Azenta Life Sciences) for next generation sequencing (NGS) or Sanger sequencing

depending on the target. The FLNA and ADAR1 target samples underwent Sanger sequencing while the FLNB target samples underwent NGS. For the FLNA and ADAR1 target samples 1 ng/µL of DNA was sent with a total mass of 10 ng. The specific primers for FLNA and ADAR1 targets (Table 2) were diluted to 5 uM and 5 µL was added to make 15 µL reaction. For the FLNB target between 100 – 500 ng of DNA was sent for Amplicon EZ sequencing. The reactions were multiplexed to increase the throughput for NGS. The primers were labelled with 1 of 6 unique 5 nucleotide barcodes. After PCR was performed, 6 samples were pooled together and purified. Each sample used a different barcoded primer (Table 5).

Sanger Sequencing Analysis. The chromatograms obtained from Sanger sequencing were analyzed with ImageJ to measure the area under the adenosine (A) and guanine (G) peaks at the edited site. After the areas of the peaks were determined the equation: percent G = (G/(G+A)) x 100 was used to calculate the percent of G nucleotides, which is equivalent to the percent of editing at that site.

NGS Analysis. The NGS FASTQ files that were received after the completion of NGS were shared with bioinformaticians at the Bioinformatic and Analysis Core of the University of Missouri for analysis. The bioinformaticians ran the FASTQ files through a computational code that sorts the sequences based on the barcodes present on the sense primers. After sorting by barcodes, the sequences that match the reference sequence from the barcode to the editing site were counted to determine the number of sequences that have either an A or G nucleotide in the editing site. The percent of sequences that have G in the editing site is equal to the percent editing for that sequence.

Change in Editing Analysis. To determine the change in editing the percent editing of the LPS treated mouse was subtracted from the percent editing of its corresponding saline treated co-housed littermate pair.

qRT-PCR

qRT-PCR was utilized to quantify expression of inflammation-induced genes. All equipment was sanitized by UV light at least 15 minutes prior to assembling reactions. The cDNA was diluted to 1:10. A master mix that contained iTaq Universal SYBR Green Supermix (Bio-Rad), forward and reverse primers, and water was created. The forward and reverse primers used were specific to GAPDH, TNFα, or MDA5. These primers were created using primerBLAST. The sequence of these primers are listed in Table 4. Eight micoliters of the master mix was aliquoted into qPCR tubes. Each qPCR reaction contained 5 µL of iTaq Supermix, 10 ng of forward primer, and 10 ng of reverse primer. Two microliters of the 1:10 cDNA dilution was pipetted into the qPCR tubes with the master mix to create a 10 µL reaction. A negative transcription control (NTC) that contained 2 µL of water instead of cDNA was also created. Each sample was done in duplicate. The reactions were placed in a Bio-Rad CFX Connect Real-Time System thermocycler with the cycling conditions outlined in Table 6.

qPCR Analysis. Each cDNA sample with RT (unknown) was compared to the corresponding no RT cDNA sample (NRT) to ensure that the NRT had a cycle threshold (CT) value of at least 5 greater than the unknown samples and/or that the peak of the NRT melt curves were distinctly different than the unknown samples.

Primer Efficiency

Cloning. In order to determine the primer efficiency of each primer pair, each target was amplified by standard PCR using DreamTaq (Thermo). The gel purified PCR products for each target were cloned into vectors using the pGEM-T Easy Vectors Systems from Promega. The ligation reactions contains T4 DNA ligase in a standard reaction (PCR product + pGemT), positive control (control insert DNA alone), and background control (pGemT alone). The contents of these reactions are listed in Table 7. These reactions were incubated for 48 hours at 4 °C. The reactions were then transformed into chemically competent (treated to promote attachment of the plasmid DNA) DH5α cells. The DH5α cells were thawed on ice for 30 minutes. One hundred microliters of the thawed cells were aliquoted into 1.5 mL tubes. Five microliters of each ligation reaction were added to the thawed cells. A negative transformation control was created that contained no DNA and a positive transformation control was created using pBluescript (pBS). The tubes were incubated on ice for 20 minutes. They were then heat shocked in a 42 °C water bath for 37 seconds and then placed on ice. Seven hundred microliters of room temperature NZY+ media was added to each tube over a flame to maintain a sterile enviroment. The tubes were then incubated at 37 °C in a shaking incubator for 1 hour. Three hundred and fifty microliters of each reaction were plated on lysogeny broth (LB) plates with a 1 X concentration of ampicillin. The plates were then incubated at 37 °C overnight. After incubation, 5 mL cultures were created from the colonies that were grown on the standard ligation reaction plate. Four cultures of 1 X ampicillin in LB broth were inoculated with a single colony picked with a sterile pipette tip. The cultures were incubate at 37 °C overnight.

Miniprep. Bacterial cultures were centrifuged at 10,000 x g for 5 minutes. The supernatant was poured off and the inverted tubes were blotted on a paper towel to dry. To each tube, 250 μL of the cell resuspension solution was added. The tubes were vortexed until the cells

were fully resuspended. Once resuspension was achieved the solution was transferred to 1.5 mL tubes. To the 1.5 mL tubes, 250 µL of the cell lysis solution was added. The tubes were inverted to mix and then incubated for 5 minutes at room temperature. Ten microliters of the alkaline protease solution was added, the tubes were inverted to mix, and then incubated for 5 minutes at room temperature. After the incubation period, 350 µL of the neutralization solution was added. Again, the tubes were inverted to mix and then centrifuged at 10,000 x g for 10 minutes. The cleared lysate was transferred to prepared spin columns inserted into 2 mL collection tubes. The collection tubes with the spin columns inserted were then centrifuged at 10,000 x g for 1 minute. The spin columns were then removed and the flow through in the collection tubes were discarded. The spin columns were inserted back into the collection tubes and 750 µL of the column wash was added. The spin columns and collection tubes were centrifuged for 1 minute at 10,000 x g. The spin columns were again removed and the flow through was discarded. The spin columns were placed back onto the collection tubes and 250 µL of the column wash was added. The tubes were centrifuged for 2 minutes and the collection tubes with the flow through were discarded. The spin columns were then inserted into new 1.5 mL tubes. One hundred microliters of nuclease free water was added to the spin column and then centrifuged for 1 minute at 10,000 x g. The spin columns were then discarded and the 1.5 mL tubes with the flow through were stored in -20 °C for further use.

Serial Dilution. The concentration of the minipreps that were prepared previously were assayed using the IMPLEN NanoPhotometer NP80 using the nuclease free water as a blank. A serial dilution was created with the highest concentration miniprep. The dilution range for the serial dilution was from stock to 1/1,000,000. qPCR was then performed on this serial dilution using the primers corresponding to the target. Each reaction was done in duplicate.

Prime Efficiency Analysis. The cycle threshold (CT) averages from the duplicate reactions were used in the determination of the primer efficiency. The averages and the log of the serial dilutions were used to create a scatter plot and the trendline was added. The R^2 value and slope of the trendline were determined. The slope of the final trendline was used to determine the efficiency using the equation $E = -1 + 10^{\wedge(-1/\text{slope})}$.

Gene Ratio Analysis. To determine the gene ratio, the E value obtained for each target was used to determine the Ep value using the equation: $Ep = E + 1$. The fold change was determined by the equation: fold change $= (Ep)^{\text{deltaCT}}$, where the deltaCT was calculated by taking the average of each target CT and subtracting that from the average of all saline samples for that target. This was done for GAPDH, TNFα, and MDA5. The gene expression ratio for TNFα and MDA5 was then calculated by dividing the fold change for TNFα or MDA5 by the GAPDH fold change. The normalized gene expression ratio for TNFα and MDA5 was then determined by finding the average of all saline gene expression ratios for the specific target and then dividing each sample's gene expression ratio by the average saline gene expression ratio.

Statistics

JASP, the open-source program supported by the University of Amsterdam, was used for all statistical analyses.

ANOVA. A classical one-way *ANOVA* was used to analyze the statistics for the expression of TNFα, MDA5, and ADAR1 p150 as well as the editing rate of FLNA and FLNB. The Levene's Test for Equality of Variances was used for the assumption check. If a homogeneity correction was needed, the Welch homogeneity test was utilized. Dunn's Post Hoc Comparisons was used to determine the p value and significant comparisons. An outlier test was performed using boxplots and the outliers were removed for the final statistical analysis.

T-Test. Independent Samples T-Tests were used to analyze the statistics of the change in editing for FLNA and FLNB. The Shapiro-Wilk Test of Normality was used for the assumption check. An outlier test was performed using boxplots and the outliers were removed for the final statistical analysis.

Table 1. Cycle conditions for HC-RT protocol

Step	Temperature	Time
1.	24°C	10:00
2.	37°C	1:00:00
3.	85°C	10:00
4.	4°C	Infinite Hold

Table 2. PCR Primers

Target	Sense (S) or Antisense (AS)	oRU #[1]	Sequence	Product Length (bp)
ADAR1 p110	S	33	AGAGACTACGCGTTGGGACTAGCC	448
ADAR1 p150	S	34	CCGGCACTATGTCTCAAGGGTTC	406
	AS	35	CCGGAAGTGTGAGCAAAGCCCGT	
FLNA	S	101	CTGATAGCCCCTTCGTGGTG	249
	AS	102	AGATGCCATTCTCTCGTGGG	
FLNB	S	116	GAGTTCAGCATCTGGACCCG	330
	AS	84	CCCTTTCGCACCATTCAACC	

---

[1] oRU refers to labels given to primers in the Ulbricht lab primer database

Table 3. Primers for potential ADAR1 editing targets

Target	Sense (S) or Antisense (AS)	oRU #	Sequence	Product Length (bp)
IGFBP7	S	141B	CTCTTCCTCCTCTTCGGATGC	582
	AS	142	AATGGCCAGATTTTCCCGGT	
IGFBP7	S	143	GGCATGGAGTGCGTGAAGAG	561
	AS	144	ATGGAGGGCATCAACCACTG	
BLCAP	S	145	CAGGTATCGTGGCGTCG	
	AS	146	ACATCACAGGCCAAAAGGCT	605
	AS	147	AAGGTTTCCGTTCCAGGAGG	332
BLCAP	S	148	GCTCGCAGGTATCGTG	567
	AS	149	GGACTGCGGGATTTGAAACT	
RPA1	S	150	CTCAGAGGGCTGTGTGTGAA	214
	AS	151	AGACAAAAAGGTGCCACCAC	

Table 4. Primers for qPCR targets

Target	Sense (S) or Antisense (AS)	oRU #	Sequence	Product Length (bp)
TNFα	S	93	ATCCTGGCCATCAAGGGCAATC	161
	AS	94	TCCCTGGGCCTCATTAGCATATCA	
GAPDH	S	109	CCCAGCTTAGGTTCATCAGG	225
	AS	113	GCCGTTGAATTTGCCGTGAG	
MDA5	S	134	GACAGAGGCCTGGAACGTAG	255
	AS	135	CAAATGGAAGTGGCCCAACC	

Table 5. PCR primer sequences for NGS

Target	oRU #	Barcode	Primer Sequence with barcode
FLNB	120	**GAGAG**	**GAGAG**GAGTTCAGCATCTGGACCCG
FLNB	121	**TTCTT**	**TTCTT**GAGTTCAGCATCTGGACCCG
FLNB	122	**CCTCC**	**CCTCC**GAGTTCAGCATCTGGACCCG
FLNB	123	**ACGCA**	**ACGCA**GAGTTCAGCATCTGGACCCG
FLNB	124	**CGTGC**	**CGTGC**GAGTTCAGCATCTGGACCCG
FLNB	125	**TACAT**	**TACAT**GAGTTCAGCATCTGGACCCG
FLNB	128	**GAGAG**	**GAGAG**CTCTCCCCTTTCGCACCATTCAACC
FLNB	129	**TTCTT**	**TTCTT**CTCTCCCCTTTCGCACCATTCAACC
FLNB	130	**CCTCC**	**CCTCC**CTCTCCCCTTTCGCACCATTCAACC
FLNB	131	**ACGCA**	**ACGCA**CTCTCCCCTTTCGCACCATTCAACC
FLNB	132	**CGTGC**	**CGTGC**CTCTCCCCTTTCGCACCATTCAACC
FLNB	133	**TACAT**	**TACAT**CTCTCCCCTTTCGCACCATTCAACC

Table 6. qPCR cycling conditions

Step	Temperature	Time
1.	95.0°C	3:00
2.	95.0°C	0:10
3.	57.0°C	0:30
	Plate Read	
4.	GOTO Step 2, 45x	
5.	65.0°C to 95.0°C, increment	0:05
	0.5°C	
	Plate Read	

END

Table 7. Ligation reaction contents

Reagents	Standard Ligation Reaction	Positive Control	Background Control
2X Rapid Ligation Buffer, T4 DNA Ligase	5 µL	5 µL	5 µL
PGEM-T Easy Vector (50 ng)	0.5 µL	0.5 µL	0.5 µL
PCR Product	3.5 µL	-	-
Control Insert DNA	-	2 µL	-
T4 DNA Ligase	1 µL	1 µL	1 µL
Water	-	1.5 µL	3.5 µL

RESULTS

The goal of this research was to determine if induced acute inflammation caused sex dependent effects on innate immunity and, consequently, ADAR-dependent RNA editing with specific interest in the innate immune pathway in skeletal muscle of mice. An acute inflammation reaction was stimulated by injecting mice with a relatively high dose of LPS and isolating tissues only 4 hours after injection. The RNA isolated from these tissues was then analyzed for gene expression and RNA editing.

Analysis of Inflammation Induction

To determine if inflammation was induced within the LPS injected mice, the relative expression levels of the pro-inflammatory cytokine TNFα were measured using qRT-PCR (Fig. 4). First, the primer efficiency of the primers used to amplify TNFα and the control, GAPDH, in qRT-PCR was analyzed (Fig. 5). The slope of the lines generated in Figure 5A and Figure 5C were used to calculate the primer efficiencies for both TNFα and GAPDH, respectively. The primer efficiency values, 1.16 for TNFα and 1.26 for GAPDH, were then used to determine the relative expression (Pfaffl 2001).

It is expected that TNFα levels would be significantly higher in the LPS injected mice compared to those that received an injection of saline. The average relative expression of TNFα in males treated with LPS was 1.13 ± 0.119, significantly higher than the average in the saline group that was 0.22 ± 0.059 ($p = 0.019$, Fig. 4). TNFα in the female LPS-treated group was also significantly higher than the saline treated females, 2.43 ± 0.389 and 0.83 ± 0.183, respectively ($p = 0.019$, Fig. 4). This confirmed inflammation was induced by LPS in both sexes. Statistical analysis of TNFα in males and females treated with LPS did not show any sex-dependent

significance, even though the female animals treated with LPS (standard deviation = 0.77) do have more than twice the amount of TNFα than the male animals treated with LPS (standard deviation = 0.24).

Analysis of ADAR1 p150 Induction

To determine the level of ADAR1 p150 induction in this research model for acute inflammation in the skeletal muscle, semi-quantitative PCR was conducted. With this method, the expression of the p150 isoform of ADAR1 relative to the constitutively expressed p110 isoform was determined by densitometry analysis from an agarose gel image of RT-PCR products (Fig. 6). Since ADAR1 p150 is IFN inducible, it was expected that the mice that were injected with LPS would have higher levels of ADAR1 p150 compared to those that received the saline injection. The average induction of ADAR1 p150 in skeletal muscle from mice in the saline groups were 10.49 ± 2.55 and 12.26 ± 1.98 for males and females, respectively. In the LPS treated muscle, ADAR1 p150 levels were 22.07 ± 4.47, and 33.87 ± 6.68, for males and females, respectively, showing ADAR1 p150 levels more than double in skeletal muscle from LPS treated mice (Fig. 7). Statistical analysis verifies that ADAR1 p150 expression is induced by LPS in both male and female mice ($p = 0.009$ and 0.006, males and females, respectively) (Fig. 7). There was not a significant difference between the sexes, however there is a significant amount of variation in the ADAR1 p150 levels in the LPS-treated females (standard deviation = 14.94) compared to the LPS-treated males (standard deviation = 8.93).

Analysis of MDA5 Expression

Next, the amount of MDA5 was quantified in both male and female mice. MDA5 activity is directly regulated by the RNA editing activity of ADAR1 p150. Based on previous literature,

female mice have higher levels of MDA5 in inflamed heart tissue (Koeing et al. 2014). MDA5

levels in the heart of the LPS treated mice were investigated (Fig. 8), as well as other tissues,

including skeletal muscle using qRT-PCR (Fig. 9). It was expected that the relative expression of

MDA5 would be higher in LPS-treated females, compared to LPS-treated males. First, the

primer efficiency of the primers used to amplify MDA5 and the control, GAPDH, in qRT-PCR

were analyzed (Fig. 5B,C respectively). The slope of the lines generated in Figure 5B and Figure

5C were used to calculate the primer efficiencies for both MDA5 and GAPDH, respectively. The

primer efficiency values, 0.83 for MDA5 and 1.26 for GAPDH, were then used to determine the

relative expression (Pfaffl 2001).

The average relative expression of MDA5 in heart tissue from mice in the male saline

group was 1.55 ± 0.61 and in the male LPS group was 10.78 ± 6.92, an increase of nearly 6 times

in the inflamed mice (Fig. 8). In the females, the MDA5 levels in LPS treated mice were over 5

times the amount in the control (relative expression in saline group was 1.66 ± 0.83, and $9.46 \pm$

3.85 in the LPS group; Fig. 8). Statistical analyses indicated that there were no significant

differences between the sexes or treatments in the heart tissue for this research model.

The average relative expression of MDA5 in skeletal muscle from mice in the male saline

group was 0.14 ± 0.07, and in the male LPS group was 0.46 ± 0.04, an increase of over 3 times

in the inflamed mice (Fig. 9). In the females, the MDA5 levels in LPS treated skeletal muscle of

mice were over 10 times the amount in the control (relative expression in saline group was 0.20

± 0.02, and 2.04 ± 0.65 in the LPS group; Fig. 9). These results indicate that MDA5 is induced

by LPS in the skeletal muscle of both sexes ($p = 0.049$ and 0.003, for males and females,

respectively). There were no statistically significant sex dependent differences for MDA5 levels

in skeletal muscle, but it is interesting to point out that, similar to TNFα and ADAR1 p150, the

variation in the females is more pronounced (standard deviation = 0.65), compared to the males (standard deviation = 0.04).

Analysis of RNA Editing

Next, the average editing rate and the change in editing of ADAR targets in skeletal muscle of both male and female LPS and saline treated mice was quantified. FLNA and FLNB mRNA are both edited in the heart and muscle. They are primarily thought to be targeted by ADAR2 in mice. While previous studies showed that inflammation in these mice did not affect levels of RNA editing in the brain or heart, it is clear that regulation of ADAR and RNA editing is tissue specific (Adetula et al. 2021; Gabay et al. 2022). Therefore, RNA editing in the skeletal muscle was analyzed as well. The average percent editing of FLNA from mice in the male saline group was 43.19% ± 1.31, and in the male LPS group was 41.35% ± 2.14 (Fig. 10A). The change in editing was calculated by analyzing the difference in FLNA editing rate between matched pairs of mice that were co-housed littermates, injected in parallel. The average change in editing for FLNA in male mice was 1.84% ± 2.39 (Fig. 10B), indicating little to no influence on FLNA editing in male mice. In female mice, editing of FLNA from control mice was 37.87% ± 2.79, and 37.53% ± 2.85 in the LPS treated group (Fig. 10A). The change in editing between paired mice was 2.54% ± 1.78 (Fig. 10B), once again indicating that acute inflammation does not significantly affect FLNA RNA editing. Interestingly, FLNA RNA editing is sex dependent in skeletal muscle (p = 0.028 and 0.021, for saline and LPS, respectively).

FLNB RNA editing rates in skeletal muscle are known to be higher than the rates in other organs. We found that the average editing percentage of FLNB editing in skeletal muscle from control mice was 72.26% ± 0.71 and 69.48% ± 2.70, in males and females, respectively (Fig. 11A). These values are higher than editing levels from the heart (65.7% and 65.5% for males and

females, respectively), but not significantly different from each other. LPS treatment had no effect on FLNB editing rate in females ($69.31\% \pm 5.09$ in LPS group compared to $69.48\% \pm 2.70$ in saline), however, editing in the male group increased to $77.38\% \pm 1.87$ ($p = 0.034$, Fig. 11A). When compared within individual pairs of mice, the average change in editing for FLNB in male mice was $5.12\% \pm 1.66$ and for females was $-0.022\% \pm 3.84$ (Fig. 11B). Note that the individual values for the change editing in females vary widely, showing almost a bimodal distribution (standard deviation = 8.59; Fig. 11B).

Analysis of ADAR1 Targets

While the role of FLNA and FLNB RNA editing in heart and muscle has been established, these are both primarily targeted by ADAR2. A protocol for analysis of FLNA and FLNB RNA editing was also established in previous theses. The editing rate of an ADAR1 target in skeletal muscle of both male and female LPS and saline treated mice was a point of interest for this research. Previously used ADAR1 target, CAPS1, has no detectible expression in muscle, so available databases were combed to find mRNAs that are targeted for RNA editing by ADAR1, but also expressed in the skeletal muscle. IGFBP7, BLCAP, and RPA1 mRNAs were selected to design and optimize RT-PCR analysis of RNA editing.

The first step in RNA editing analysis is to use RT-PCR to amplify the region that contained the edited nucleotide. Primers were designed to flank the edited nucleotide in the cDNA. Next, the conditions of the PCR were optimized. A melting temperature (Tm) gradient was utilized to determine the highest Tm that produced an amplicon at the expected size with minimal background for each target. The first primer set tested, oRU 141B and 142, targeted IGFBP7. The expected product size was 582 base pairs. The second set of primers tested that target IGFBP7 was oRU 143 and 144. The expected product size was 561 base pairs. After

conducting the Tm gradient and visualizing the results with agarose gel electrophoresis for both pairs of primers it was determined that the optimal Tm for both pairs of primers was 60 °C. RT-PCR was then conducted on skeletal muscle samples using 60 °C as the annealing temperature.

The next step of RNA editing analysis is to sequence the RT-PCR amplicon in skeletal muscle samples. Amplicons from IGFBP7 were sequenced with Sanger using one of the PCR primers (oRU 141B, 142, 143, or 144) to determine which primer would result in clean chromatograms. After analyzing the results of the chromatograms of all the primers, it was determined that oRU 141B and 142 both produced clean chromatograms, however, the editing site identified in previous literature appeared to be 100% edited in samples with either primer (Figure 12A,B respectively).

The next sets of primers analyzed were oRU 145 and 146, 145 and 147, and 148 and 149. These primer sets all targeted BLCAP. A Tm gradient was again utilized to determine the optimal Tm for each set of primers. Primer set oRU 145 and 146 as well as set oRU 148 and 149 were unable to produce clean bands when visualized using agarose gel electrophoresis. oRU set 145 and 147 created an optimal band at the expected target size, 330 base pairs, with a Tm of 60 °C. RT-PCR was conducted on skeletal muscle samples using 60 °C as the annealing temperature. These amplicons were then prepared with either oRU 145 or 147 and sent for Sanger sequencing. After analyzing the results of the chromatograms, it was decided that oRU 145 produced cleaner chromatograms, however, the edited site identified in previous literature appeared to not be edited in any samples (Fig. 12C).

The next set of primers tested was oRU 150 and 151. This primer set targeted RPA1. Again, a Tm gradient was used to determine the optimal Tm for each set of primers. A Tm of 63.8 °C produced a clean band at the expected size of 214 base pairs. RT-PCR was then

conducted with an annealing temperature of 63.8 °C on skeletal muscle samples. The amplicons

were then prepared for sequencing with either oRU 150 or 151 and sent for Sanger sequencing.

After analyzing the results of the chromatograms, it was determined that oRU 151 produced

clean chromatograms with the edited nucleotide present (Fig. 12D). The editing rate for RPA1 is

approximately 75%, a rate that is detectible, yet not saturated. RPA1 was determined to be a

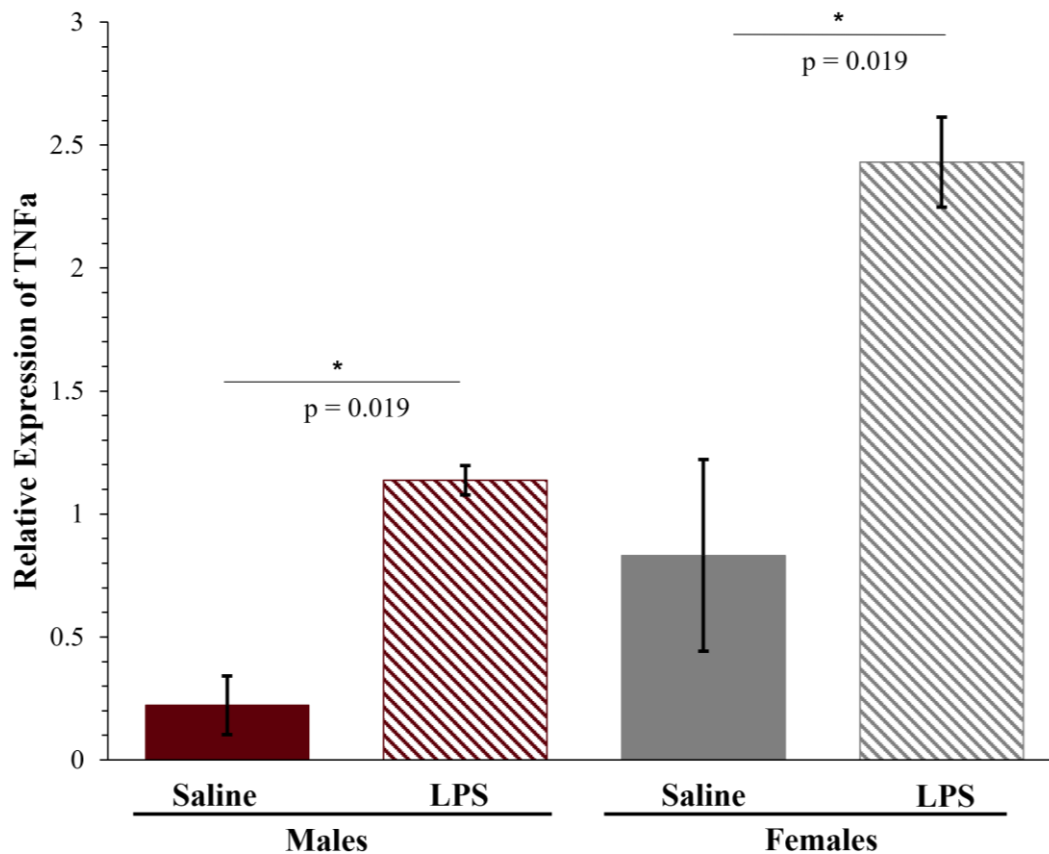satisfactory target for further analysis in future studies.

Figure 4. TNFα expression in skeletal muscle of males and females.
Relative expression was determined by qRT-PCR of TNFα from skeletal muscle, using GADPH
as a standard. Each qPCR was performed in duplicate. The Pfaffl method was used to determine
the relative expression. Male (maroon) and female (gray) mice from saline (solid) and LPS
(hatched) treated groups were tested. *ANOVA.* * p < 0.05, *** p < 0.001. Error bars equal the
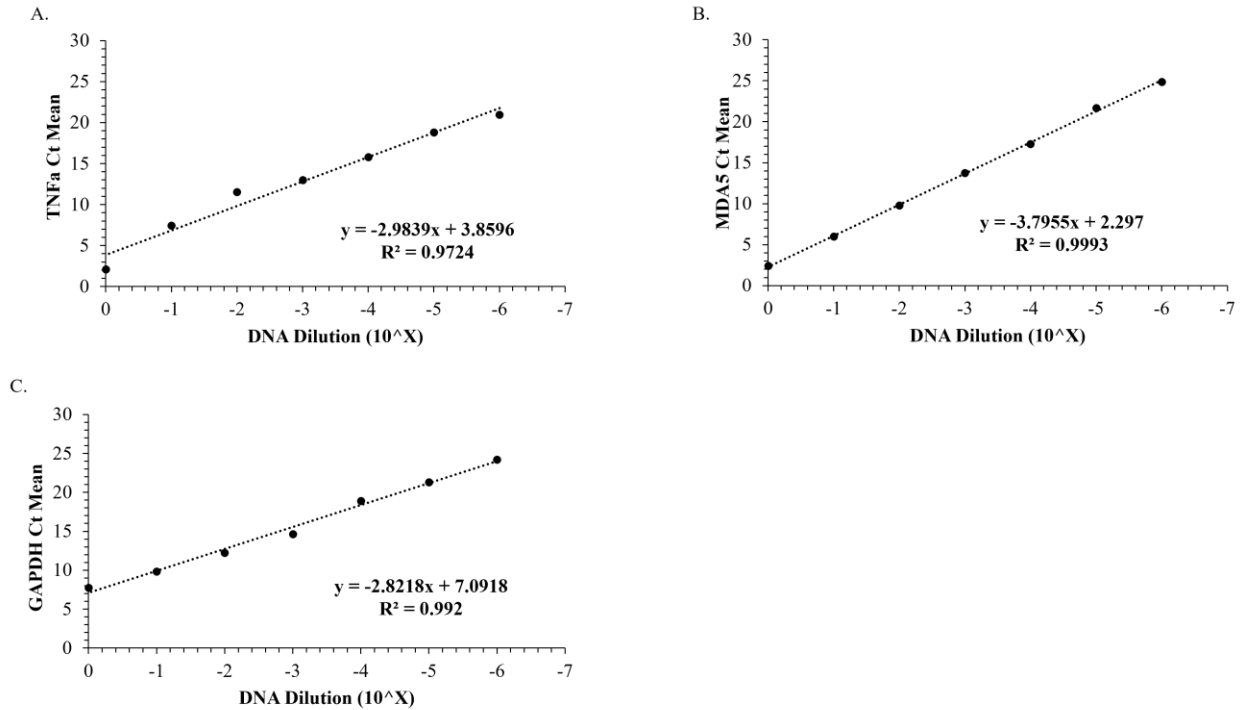standard error of the mean (SEM). N = 3 (males) or 4 (females).

Figure 5. Primer efficiency.
Serial dilutions of cloned PCR products were prepared (from 10^{-6} to stock). qPCR was performed in duplicate. The mean Ct was used to prepare the standard curves. The correlation coefficient (R-squared values) and equations of the trendline are present on each respective graph. (A) Standard curve for TNFα qPCR. (B) Standard curve for MDA5. (C) Standard curve for GAPDH.
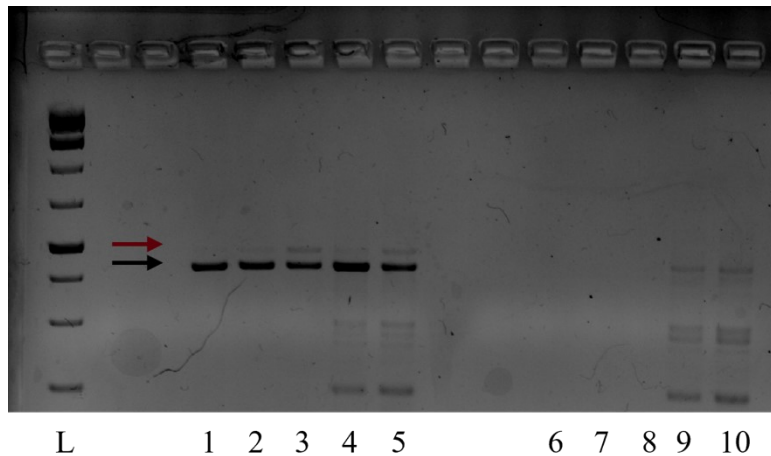

Figure 6. ADAR1 p150 agarose gel.
Representative agarose gel electrophoresis used to quantify ADAR1 p150 expression levels relative to ADAR1 p110 expression levels. The ADAR1 p110 band is indicated with a maroon arrow and the ADAR1 p150 band is indicated with a black arrow. The lane labelled "L" contained the 1kb ladder. Lanes labelled 1-5 amplified from cDNA and lanes 6-10 contain products of -RT controls.
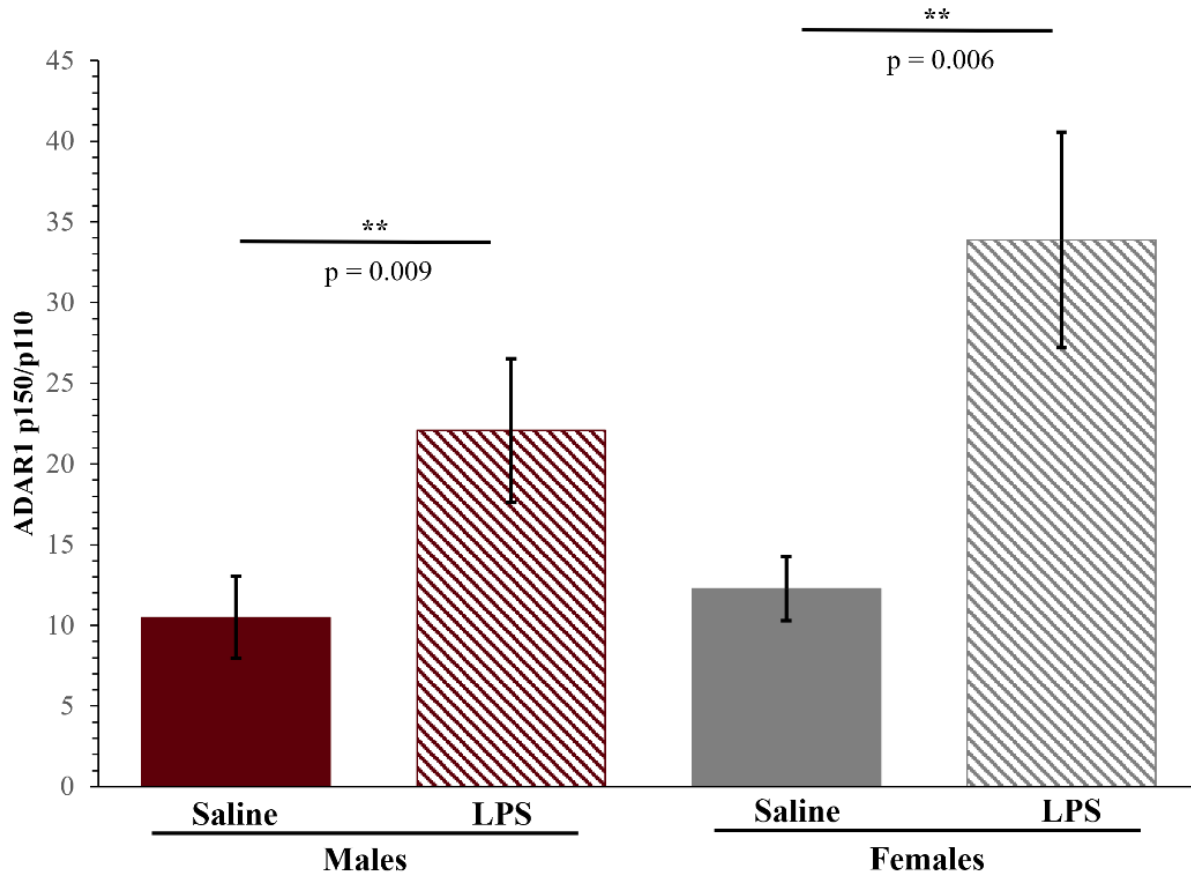
Figure 7. ADAR1 p150 expression in skeletal muscle of males and females.
Relative expression was determined by semi-quantitative PCR of ADAR1 p150 from skeletal muscle, using ADAR1 p110 as a standard. Male (maroon) and female (gray) mice from saline (solid) and LPS (hatched) treated groups were tested. *ANOVA.* ** $p < 0.01$. Error bars = SEM. n males, saline = 6; n males, LPS = 4; N females = 5.
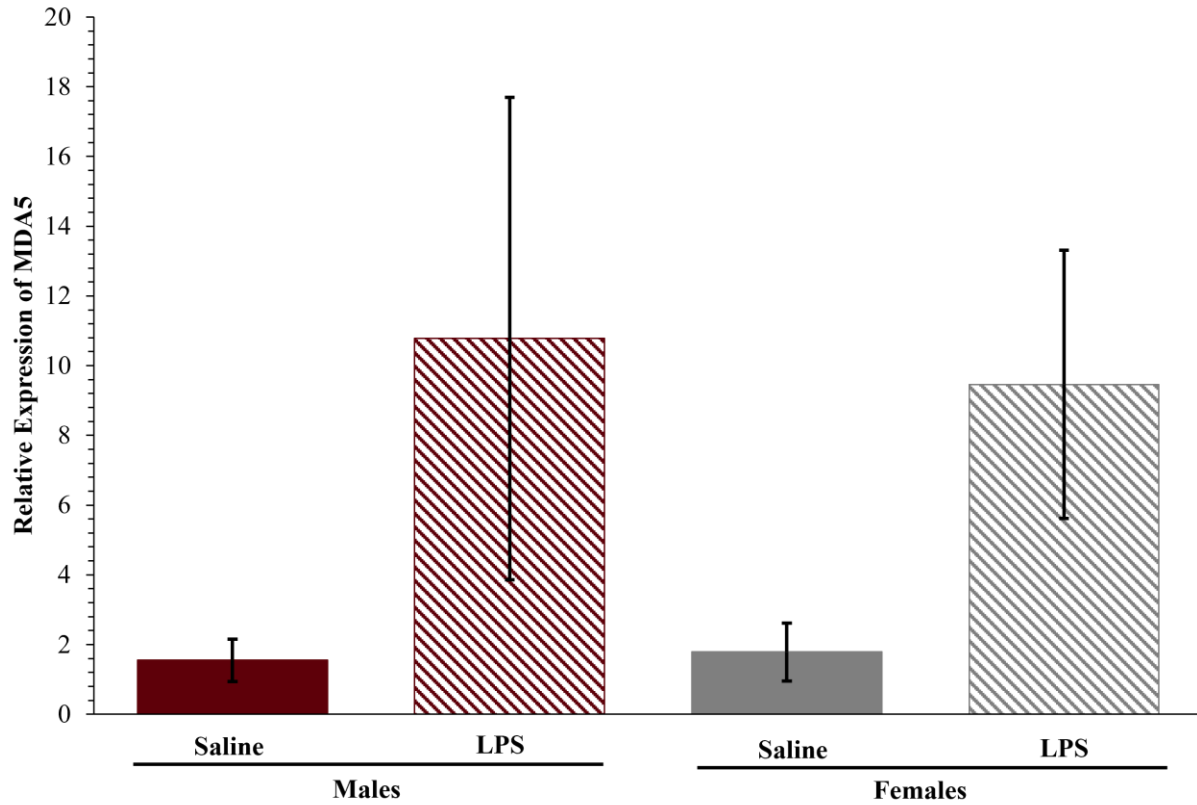
Figure 8. MDA5 expression in heart of males and females.
Relative expression was determined by qRT-PCR of MDA5 from heart, using GADPH as a standard. Each qPCR was performed in duplicate. The Pfaffl method was used to determine the relative expression. Male (maroon) and female (gray) mice from saline (solid) and LPS (hatched) treated groups were tested. *ANOVA.* (n.s.). Error bars = SEM. N = 3 (males) or 4 (females).
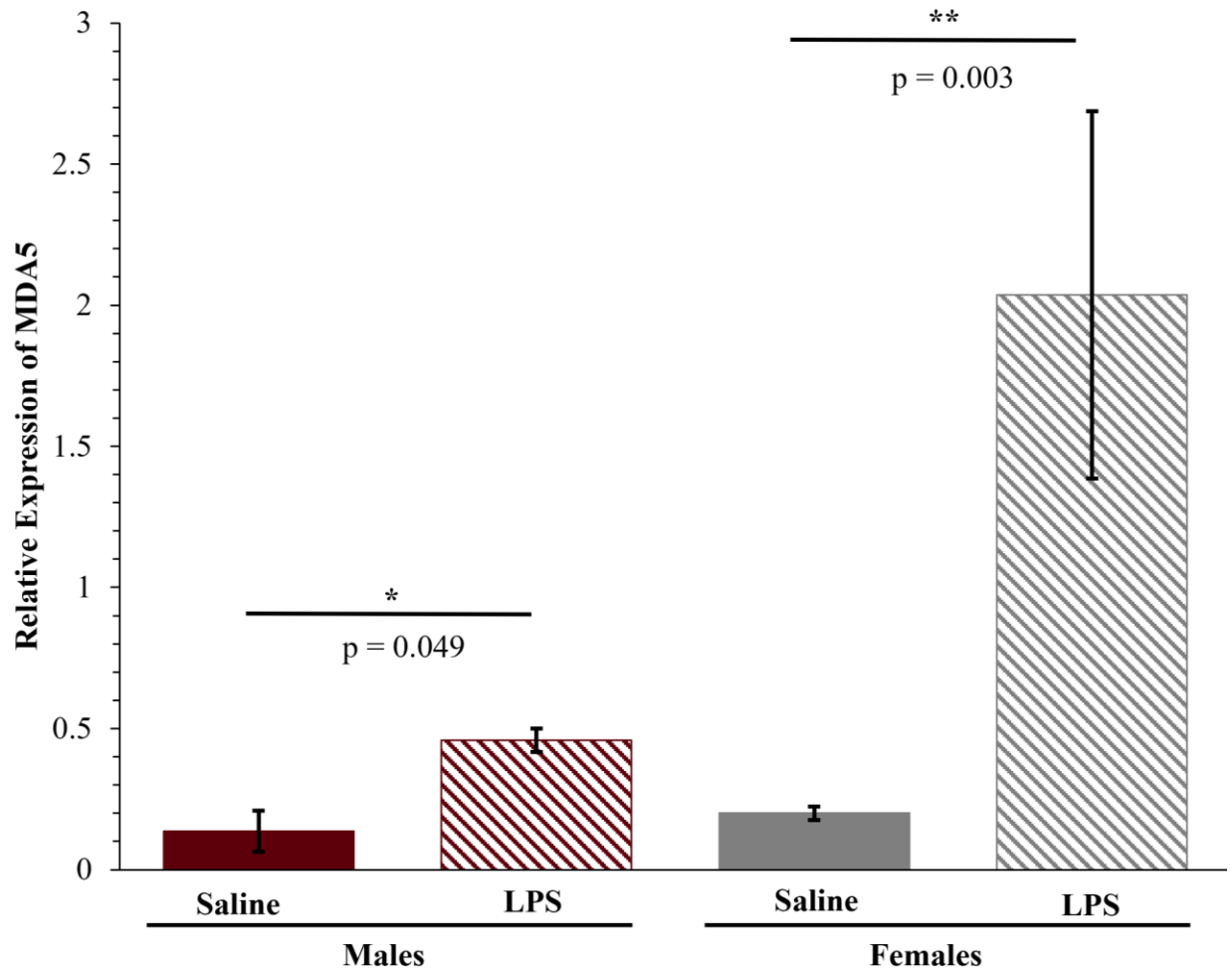
Figure 9. MDA5 expression in skeletal muscle of males and females.
Relative expression was determined by qRT-PCR of MDA5 from skeletal muscle, using GADPH as a standard. Each qPCR was performed in duplicate. The Pfaffl method was used to determine the relative expression. Male (maroon) and female (gray) mice from saline (solid) and LPS (hatched) treated groups were tested. *ANOVA*. * $p < 0.05$, ** $p < 0.01$. Error bars = SEM. N = 4 (males and females).

Figure 10. RNA Editing of FLNA in the skeletal muscle of male and female mice.
(A) Average percent editing of FLNA in the skeletal muscle of males (maroon) and females (gray) in both saline (solid) and LPS (hatched) treated groups. *ANOVA,* * $p > 0.05$. (B) The change in editing of FLNA in the skeletal muscle between LPS and saline treated co-housed littermate pairs in female (gray) and male (maroon) animals. *T-test,* $p > 0.05$ (n.s.). Error bars = SEM. N = 7 (males) or 5 (females); technical replicates $\geq$ 2.
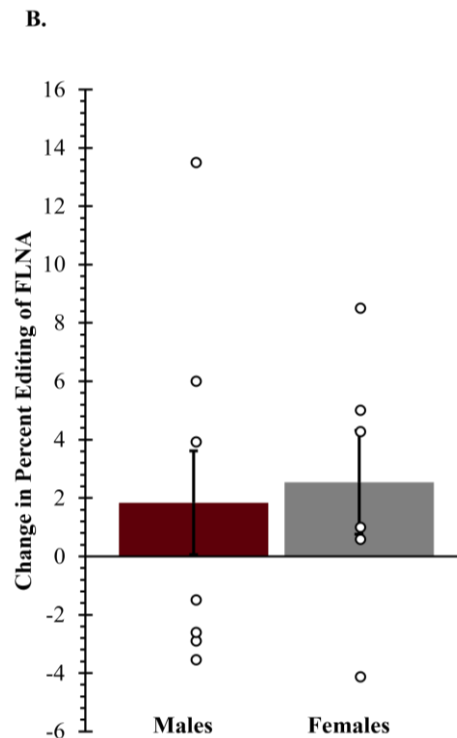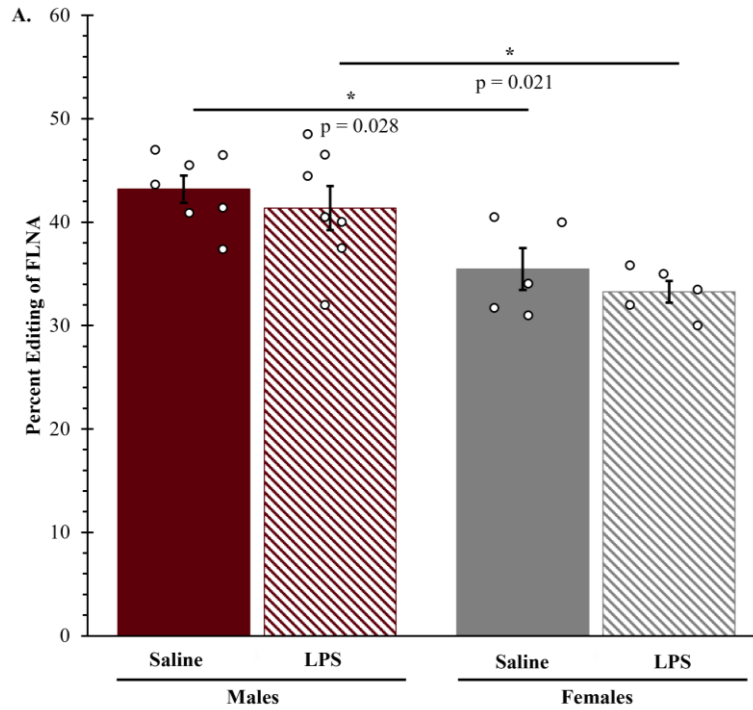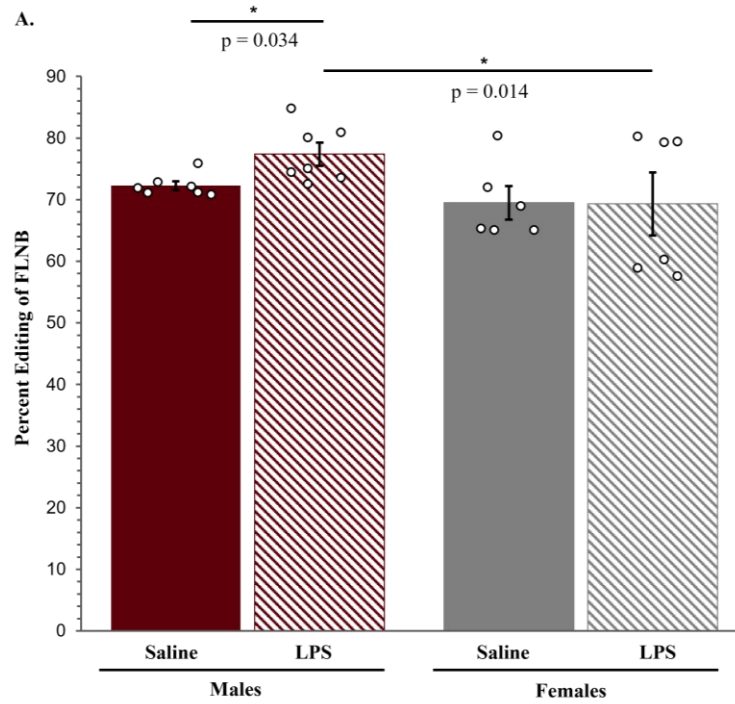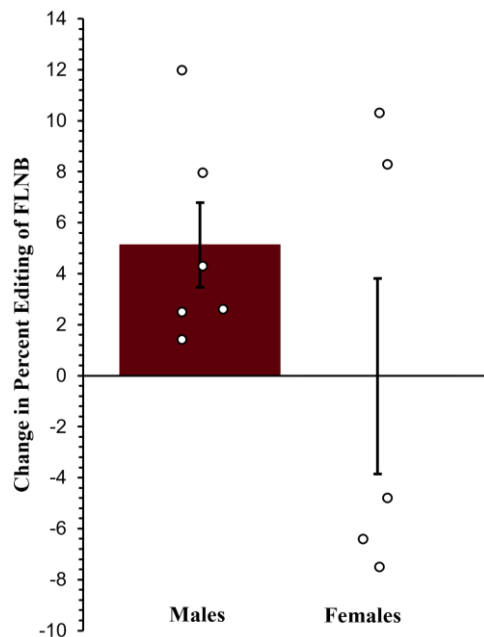
Figure 11. RNA Editing of FLNB in the skeletal muscle of male and female mice.
(A) Average percent editing of FLNB in the skeletal muscle of males (maroon) and females
(gray) in both saline (solid) and LPS (hatched) treated groups. *ANOVA,* * p > 0.05, ** p > 0.01.
(B) The change in editing of FLNB in the skeletal muscle between LPS and saline treated co-
housed littermate pairs in female (gray) and male (maroon) animals. *T-test,* p > 0.05 (n.s.). Error
bars = SEM. N = 7 (males) or 6 (females); technical replicates ≥ 2.

Figure 12. Representative chromatograms for ADAR1 editing targets.
Representative chromatograms from Sanger sequencing for the editing region of (A) IGFBP7 with oRU 141B, (B) IGFBP7 with oRU 142, (C) BLCAP, and (D) RPA1. The edited nucleotide is highlighted with a red box for all targets. G = Black, A = green, T = red, C = blue.

DISCUSSION

The goal of this research was to induce acute inflammation and examine the innate immune reaction as well as ADAR-dependent RNA editing in 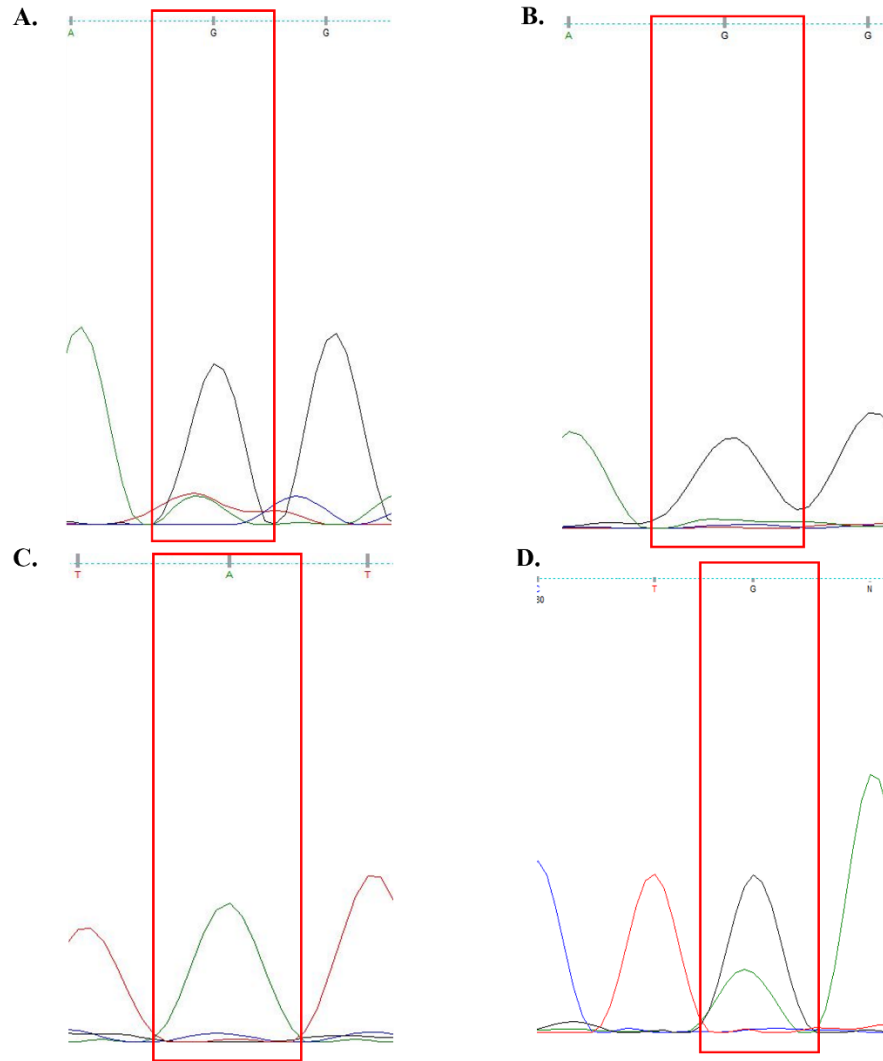mice. An acute inflammation reaction was stimulated through an injection of a relatively high dose of LPS. Tissues were isolated just 4 hours after injection and the RNA isolated, with the intention of capturing the molecular signature of extremely acute inflammation. Inflammation was confirmed through the significant increase of TNFα seen in both male and female mice that were injected with LPS compared to their co-housed littermates that were injected with saline (control group) (Fig. 4). The expression of the interferon-inducible p150 isoform of ADAR1 was determined through semi-quantitative PCR. The results indicated a significant increase in the expression for both male and female mice injected with LPS when compared to the control (Fig. 7). MDA5 gene expression in the heart tissue showed no significant differences between the LPS and control groups of either males or females (Fig. 8). In the skeletal muscle there was a significant increase in MDA5 gene expression between the LPS and control groups for both sexes (Fig. 9). However, there was no statistically significant difference between the sexes. The editing of FLNA, FLNB, RPA1, BLCAP, and IGFBP7 were analyzed through Sanger sequencing or NGS. For FLNA, there was a significant difference in percent editing between the males and females for both the LPS and saline treated mice (Fig. 10A). However, there was no treatment difference for either sex as well as no significant difference in the change in editing between males and females (Fig. 10A,B respectively). The editing rate for FLNB also indicated a significant difference between the sexes for the LPS treated mice (Fig. 11A). There was also a significant difference of editing rate in treatment groups for the males, but not for the females (Fig. 11A). Like FLNA, there was no difference in the change in editing between pairs of males and females for FLNB (Fig. 11B).

42

IGFBP7, BLCAP, and RPA1 were all analyzed to determine which target would provide optimal conditions for analysis of RNA editing of an ADAR1 target (Fig. 12). IGFBP7 demonstrated 100% editing regardless of the conditions (LPS vs. saline or males vs. females) making the effects of inflammation on RNA editing of this target impossible to determine for this model. BLCAP demonstrated 0% editing regardless of the conditions, also making the effects of inflammation on RNA editing of this target impossible to determine for this model. RPA1 is an ADAR1 target, demonstrated a variable editing rate, and is likely to be useful for further analysis (Fig. 11).

Induction of Immune Related Genes

The confirmation of induced inflammation in skeletal muscle was determined by quantifying the induction of interferon stimulated genes like TNFα, ADAR1 p150, and MDA5. qRT-PCR was used to quantify the relative gene expression of TNFα, a pro-inflammatory cytokine. All LPS treated mice had increased gene expression of TNFα in the skeletal muscle, as expected. The female LPS treated mice did show over double the amount of TNFα when compared to the male LPS treated mice, however, this difference was not statistically significant. This could be due to the larger variance seen with the female mice when compared to the male mice (Fig. 4).

The induction of ADAR1 p150 was investigated using semi-quantitative PCR, normalizing to the constitutive p110 isoform of ADAR1. It is important to note that the expression of the constitutively active isoform ADAR1 p110 was assumed to not change. Confirmation of these assumptions should be done by qRT-PCR of the p110 isoform in future experiments. For all mice, the expression of ADAR1 p150 was higher in the LPS treated group (Fig. 7). Since the p150 isoform of ADAR1 is interferon inducible these results were expected

43

after confirmation of inflammation was determined. Like TNFα the female mice exhibited over double the amount of ADAR1 p150 expression, however no significant differences were found between the sexes. This is most likely also due to the females having a larger variance compared to the males.

MDA5 is a dsRNA sensor that, when triggered, leads to the induction of inflammation. The function of MDA5 is downregulated by ADAR1 p150, in a negative feedback loop, to prevent dysregulation of the immune system and chronic induction of inflammation. Co-regulation of the levels of ADAR1p150 and MDA5 help keep innate immunity in check, preventing activation by endogenous dsRNA. Previous literature has shown a significant increase of MDA5 in inflamed heart tissue of females compared to males (Koenig et al. 2014). This research aimed to confirm those findings in the heart in this acute inflammation model, as well as investigate if there is a similar pattern of differential MDA5 expression in the skeletal muscle. The acute inflammation model investigated in this research did not imitate the previous significant differences seen in inflamed heart tissues of female when compared to males (Fig. 8). The sample size for this research is relatively low for MDA5 from the heart (male n = 3). Analysis of additional samples may reduce the variability and provide a more accurate picture of MDA5 in the heart. However, the extremely acute inflammation model (4 hours) used for this research is much different than the 3-day acute inflammation model found in previous research. To determine if the inflammation induced in this research leads to significantly higher levels of MDA5 in the heart tissue of females and supports the previous findings an extended time of inflammation could be tested in future research. The acute inflammation model here did, however, induce a significant increase in MDA5 expression in the skeletal muscle of both males and females (Fig. 9). While there was not a statistically significant difference between the sexes

it appears that the differences are approaching significance. Again, the female LPS group showed over double the amount of MDA5 expression when compared to the male LPS group, and the variability follows the trend of the other ISGs investigated, with females exhibiting higher variance. The sex-dependent differences of MDA5 induction have not been previously investigated in tissues other than the heart. To determine if this model is in fact approaching significance in the skeletal muscle more samples should be tested in an attempt to decrease the amount of variance. Furthermore, testing longer periods of inflammation could also provide more insight on the sex-dependent differences of induction.

The results of the induction of immune related genes in skeletal muscle of mice that were investigated in this research all indicate a significant increase following LPS injections, indicating that the timing and dose of LPS successfully induced immune activation. Interestingly, they all also follow the same trend of the expression being over double the amount in females when compared to males, but none indicating any statistically significant difference between the sexes. Since the females displayed larger variance for each target studied it may be worthwhile to increase the number of mice used to decrease the variance to portray the significant difference between the sexes. It would also be worth investigating longer periods of inflammation since it is possible that 4 hours was not enough time to induce a large enough difference between males and females in the expression of the immune related genes, as mentioned above. Alternatively, protein expression for all targets could also be quantified by western blot with antibodies specific to the target proteins to determine if the mRNA expression correlates with the protein expression. RNA was isolated from tissues using Tri-Reagent, a phenol-based solution that separates RNA in the aqueous fraction from an organic fraction, containing proteins. Protein can be isolated from this stored organic fraction using dialysis. Total protein can be separated by

SDS-polyacrylamide gel electrophoresis and blotted to nitrocellulose. Primary antibodies recognizing each target should be thoroughly analyzed to ensure they are specific and sensitive enough to detect the intended targets. Secondary antibodies labeled with an infrared dye can be used to visualize protein levels. Once that has been accomplished, the software ImageJ could be used to quantify the protein levels. If the protein levels are not induced to the same levels as the mRNA, then it could be that the 4-hour time point was not sufficient time for the production of the protein and again, an extended inflammation period should be studied to further determine if the sex differences are significant.

RNA Editing in Skeletal Muscle

Previous research conducted by gradute student Claire Nichols aimed to investigate the effects of inflammation on RNA editing and determine if the effects are tissue and/or sex-specific in the heart, brain, and skeletal muscle of saline and LPS treated mice. The editing targets that were examined included FLNA, FLNB, and CAPS1. The data collected did not show a significant difference in editing between the LPS and saline treated mice, nor a sex-specific difference, for any of the targets in the heart and brain tissue. Preliminary data on FLNA in skeletal muscle, however, did show that editing was reduced by inflammation and that editing in female mice was reduced for both saline and LPS treated groups when compared to males. This research aimed to confirm these results as well as investigate other targets in skeletal muscle.

This thesis research expanded the previous project and provided additional samples for FLNA editing in LPS and saline treated skeletal muscle of male and female mice, showing a slight reduction but no statistcally significant difference between the treatment groups. However, this research did support the preliminary data that indicated a significant decrease of about 5% in the editing of FLNA in skeletal muscle of female mice for both the saline and LPS treated groups

when compared to males (Fig. 10A). The change in editing between age-matched, co-housed littermates that were injected with LPS or saline, in parallel for males and females however was not significantly different (Fig. 10B). This indicates that for FLNA, the effects of inflammation on editing percent are tissue dependent but not sex-dependent, meaning the regulators of FLNA editing, such as transcription rate, splicing rate, or RNA binding proteins might vary between tissues.

FLNB editing levels have been shown to be the highest in skeletal muscles, cartilage, and bones where the function of FLNB seems to be the most important (Czermak et al. 2018). Given this information, determining how/if inflammation affects RNA editing of FLNB in the skeletal muscle even though there were no significant differences found in the heart and brain was deemed important. The data collected from this research did not show a significant difference in the change in editing between age-matched, co-housed littermates that were injected with LPS or saline, in parallel (Fig. 11B). However, LPS led to a statistically significant difference in the editing percentage of FLNB in male mice. The male mice displayed a significant increase in editing in the samples that were treated with LPS compared to the control male mice and the LPS-treated female mice. The females did not show a treatment difference, and the FLNB editing in all female mice was very similar to the control male mice (Fig. 11A).

The FLNB editing rate was higher in the male LPS treated mice than all other groups (Fig. 11A). This is interesting when coupled with the data collected from the induction of immune related gene expression. As stated above, for each immune related gene target, the females that were treated with LPS exhibited more than double the expression when compared to males, however the editing of FLNB in females did not show any significant difference after the treatment of LPS while the males displayed higher editing in the LPS group. This indicates that

regardless of the cellular conditions, FLNB editing is maintained at a steady level in female mice. The slight variability in the males indicates that more of the FLNB protein produced in the LPS treated males would contain arginine instead of glutamate at amino acid 2341 (Levanon et al. 2005). The editing-dependent change in amino acid for FLNA affects smooth muscle constriction in cardiovascular tissue, where the majority of editing has been found for FLNA. Under-editing of FLNA has been found in cardiovascular tissue from humans and mice with cardiovascular diseases. When the editing of FLNA was impaired in mice, there was more contractility of the smooth muscle that leads to diastolic hypertension (Jain et al. 2018). The majority of FLNB editing has also been found in skeletal muscle. Editing of FLNB, which affects the same amino acid at the same position as FLNA, may similarly affect contractility of skeletal muscle (Czermak et al. 2018). We expect a temporary change in editing to minimally affect the tissue, and therefore be well tolerated by the animal. However, if more sustained inflammation causes sustained increases in FLNB editing in males, it is possible that the alternative FLNB isoform could reduce contractility and affect the overall function of the musculoskeltal sytem.

It is important to note that FLNA and FLNB are primarily ADAR2 targets. ADAR1 will competitively inhibit ADAR2-specific RNA editing. Since ADAR1 p150 levels increased for both sexes in the LPS treated tissue it was expected that if ADAR1 p150 induction affected the editing of ADAR2 targets, the editing would decrease. After the quantification of ADAR1 p150 showed that the induction in females was double the amount of males, it was thought that the editing of FLNB in females injected with LPS may be reduced compared to females injected with saline as well as the males since the increased amount of ADAR1 p150 could lead to increased competitive inhibition of ADAR2. The data collected did not meet this expectation. In

fact, editing of FLNB was actually increased in conditions where ADAR1 was higher in the skeletal muscle of males only, suggesting that FLNB may indeed be edited by ADAR1. Alternatively, perhaps the conditions that stimulate ADAR1 p150 also stimulate a change in other factors that contribute to FLNB RNA editing in male skeletal muscle. One factor that could influence the level of FLNB RNA edting is its transcription rate. Higher levels of transcription are associated with lower levels of RNA editing (Saldi et al. 2021). Therefore, it could be beneficial to quantify the amount of FLNB with qRT-PCR in skeletal muscle of LPS and saline treated male and female mice to determine if the inflammation is stimulating the transcription of FLNB in males, thereby influencing it's editing rate, indirectly. Furthermore, quantification of ADAR2 expression by qRT-PCR between males and females in inflammed skeletal muscle should also be performed to determine if levels of ADAR2 could be affected, influencing the editing rate of FLNB. The protein levels of each immune related gene should also be quantified. If the protein levels do not correlate with the increased mRNA levels this could help explain the diconnect between the expected and observed results.

This work intended to measure RNA editing of ADAR1- and ADAR2-targeted transcripts. We continued previous thesis research and investigated the effects of inflammation on the ADAR2 targets FLNA and FLNB. However, Claire Nichols also investigated the ADAR1 target CAPS1. CAPS1 RNA editing was not affected by sex or LPS treatment in the heart or brain. CAPS1 is not expressed in skeletal muscle so this research aimed to determine an ADAR1 editing target that was expressed in skeletal muscle to determine how inflammation effects ADAR1 editing activity. After looking through previous literature to find ADAR1 targets, many trials of primer optimization, and Sanger sequencing test runs it was determined that RPA1 could prove to be a viable target for determining the effects of inflammation on ADAR1 editing

activity. The results for this target are not complete. Based on the results of the ADAR1 editing

activity that were seen in Claire's research it is assumed that there will not be a significant

difference in the editing percentage, but it will still be worthwhile to confirm these assumptions

and compare the results to the editing activity of ADAR2 that was seen in inflammed skeletal

muscle. If there are no differences seen in the editing rate of an ADAR1 target it can be assumed

that the editing performed by ADAR1 and ADAR2 are differentially affected by inflammation.

The previous editing targets that have been mentioned are all well known and well

regulated recoding events. It would also be important to look at how inflammation affects hyper-

editing rates. Hyper-editing is much more common than recoding editing events and are the

primary type of editing that controls the innate immune reaction (Tossberg et al. 2020). Sex

differences in the innate immune system may be more likely to be affected by or affect hyper-

editing levels. Hyper-editing levels can be assessed through RNAseq or by surveying overall

cellular levels of inosine (Knutson et al. 2021).

The results of this research, combined with those of previous and future research, helps to

highlight the complexity of RNA editing and the effects that inflammation has on the molecular

events within the cell that regulate the health and function of organ systems. This work shows

that each organ, each target and each sex may be regulated uniquely, making the results of

disturbing the satus quo increasingly unpredictible. The therapeutic potential of RNA editing is

currently being realized by targeting endogenous ADARs to disease-causing locations (Booth et

al. 2023). This targeted recoding has the potential to reduce the harm caused by genomic

mutations, but carry far less risk than genome editing strategies. However, in the discussion of

using ADAR-directed RNA editing as a therapeutic treatment, it is important to consider that

ADAR activity is sex-, tissue-, target-, and treatment-dependent. This research is the first to

investigate and demonstrate the sex-dependent nature of RNA editing and further establishes the need to involve both males and females in research, including trials for pharmeceuticals related to RNA editing-based therapeutics.

REFERENCES

Abdullah M, Chai P-S, Chong M-Y, Tohit ERM, Ramasamy R, Pei CP, Vidyadaran S. 2012. Gender effect on in vitro lymphocyte subset levels of healthy individuals. *Cell Immunol* **272**: 214–219. http://dx.doi.org/10.1016/j.cellimm.2011.10.009.

Adetula AA, Fan X, Zhang Y, Yao Y, Yan J, Chen M, Tang Y, Liu Y, Yi G, Li K, et al. 2021. Landscape of tissue-specific RNA Editome provides insight into co-regulated and altered gene expression in pigs (Sus-scrofa). *RNA Biol* **18**: 439–450. http://dx.doi.org/10.1080/15476286.2021.1954380.

Anantharaman A, Gholamalamdari O, Khan A, Yoon J-H, Jantsch MF, Hartner JC, Gorospe M, Prasanth SG, Prasanth KV. 2017. RNA-editing enzymes ADAR1 and ADAR2 coordinately regulate the editing and expression of Ctn RNA. *FEBS Lett* **591**: 2890–2904. http://dx.doi.org/10.1002/1873-3468.12795.

Aristizábal B, González Á. 2013. *Innate immune system*. El Rosario University Press https://www.ncbi.nlm.nih.gov/books/NBK459455/ (Accessed April 24, 2023).

Banerjee S, Barraud P. 2014. Functions of double-stranded RNA-binding domains in nucleocytoplasmic transport. *RNA Biol* **11**: 1226–1232. http://dx.doi.org/10.4161/15476286.2014.972856.

Barraud P, Allain FH-T. 2012. ADAR proteins: double-stranded RNA and Z-DNA binding domains. *Curr Top Microbiol Immunol* **353**: 35–60. http://dx.doi.org/10.1007/82_2011_145.

Bass BL. 2002. RNA editing by adenosine deaminases that act on RNA. *Annu Rev Biochem* **71**: 817–846. http://dx.doi.org/10.1146/annurev.biochem.71.110601.135501.

Berger I, Winston W, Manoharan R, Schwartz T, Alfken J, Kim YG, Lowenhaupt K, Herbert A, Rich A. 1998. Spectroscopic characterization of a DNA-binding domain, Z alpha, from the editing enzyme, dsRNA adenosine deaminase: evidence for left-handed Z-DNA in the Z alpha-DNA complex. *Biochemistry* **37**: 13313–13321. http://dx.doi.org/10.1021/bi9813126.

Booth BJ, Nourreddine S, Katrekar D, Savva Y, Bose D, Long TJ, Huss DJ, Mali P. 2023. RNA editing: Expanding the potential of RNA therapeutics. *Mol Ther*. http://dx.doi.org/10.1016/j.ymthe.2023.01.005.

Burns CM, Chu H, Rueter SM, Hutchinson LK, Canton H, Sanders-Bush E, Emeson RB. 1997. Regulation of serotonin-2C receptor G-protein coupling by RNA editing. *Nature* **387**: 303–308. http://dx.doi.org/10.1038/387303a0.

Chater TE, Goda Y. 2014. The role of AMPA receptors in postsynaptic mechanisms of synaptic

plasticity. *Front Cell Neurosci* **8**: 401. http://dx.doi.org/10.3389/fncel.2014.00401.

Chen CX, Cho DS, Wang Q, Lai F, Carter KC, Nishikura K. 2000. A third member of the RNA-specific adenosine deaminase gene family, ADAR3, contains both single- and double-stranded RNA binding domains. *RNA* **6**: 755–767. http://dx.doi.org/10.1017/s1355838200000170.

Chiang DC, Li Y, Ng SK. 2020. The Role of the Z-DNA Binding Domain in Innate Immunity and Stress Granules. *Front Immunol* **11**: 625504. http://dx.doi.org/10.3389/fimmu.2020.625504.

Cojocaru M, Cojocaru IM, Silosi I, Vrabie CD. 2011. Manifestations of systemic lupus erythematosus. *Maedica* **6**: 330–336. https://www.ncbi.nlm.nih.gov/pubmed/22879850.

Czermak P, Amman F, Jantsch MF, Cimatti L. 2018. Organ-wide profiling in mouse reveals high editing levels of Filamin B mRNA in the musculoskeletal system. *RNA Biol* **15**: 877–885. http://dx.doi.org/10.1080/15476286.2018.1480252.

Desterro JMP, Keegan LP, Lafarga M, Berciano MT, O'Connell M, Carmo-Fonseca M. 2003. Dynamic association of RNA-editing enzymes with the nucleolus. *J Cell Sci* **116**: 1805–1818. http://dx.doi.org/10.1242/jcs.00371.

Dias Junior AG, Sampaio NG, Rehwinkel J. 2019. A Balancing Act: MDA5 in Antiviral Immunity and Autoinflammation. *Trends Microbiol* **27**: 75–85. http://dx.doi.org/10.1016/j.tim.2018.08.007.

Feng Y, Sansam CL, Singh M, Emeson RB. 2006. Altered RNA editing in mice lacking ADAR2 autoregulation. *Mol Cell Biol* **26**: 480–488. http://dx.doi.org/10.1128/MCB.26.2.480-488.2006.

Fitzgerald LW, Iyer G, Conklin DS, Krause CM, Marshall A, Patterson JP, Tran DP, Jonak GJ, Hartig PR. 1999. Messenger RNA editing of the human serotonin 5-HT2C receptor. *Neuropsychopharmacology* **21**: 82S–90S. http://dx.doi.org/10.1016/S0893-133X(99)00004-4.

Fritz J, Strehblow A, Taschner A, Schopoff S, Pasierbek P, Jantsch MF. 2009. RNA-regulated interaction of transportin-1 and exportin-5 with the double-stranded RNA-binding domain regulates nucleocytoplasmic shuttling of ADAR1. *Mol Cell Biol* **29**: 1487–1497. http://dx.doi.org/10.1128/MCB.01519-08.

Gabay O, Shoshan Y, Kopel E, Ben-Zvi U, Mann TD, Bressler N, Cohen-Fultheim R, Schaffer AA, Roth SH, Tzur Z, et al. 2022. Landscape of adenosine-to-inosine RNA recoding across human tissues. *Nat Commun* **13**: 1184. http://dx.doi.org/10.1038/s41467-022-28841-4.

George CX, Ramaswami G, Li JB, Samuel CE. 2016. Editing of Cellular Self-RNAs by

Adenosine Deaminase ADAR1 Suppresses Innate Immune Stress Responses. *J Biol Chem* **291**: 6158–6168. http://dx.doi.org/10.1074/jbc.M115.709014.

George CX, Samuel CE. 1999a. Characterization of the 5'-flanking region of the human RNA-specific adenosine deaminase ADAR1 gene and identification of an interferon-inducible ADAR1 promoter. *Gene* **229**: 203–213. http://dx.doi.org/10.1016/s0378-1119(99)00017-7.

George CX, Samuel CE. 1999b. Human RNA-specific adenosine deaminase ADAR1 transcripts possess alternative exon 1 structures that initiate from different promoters, one constitutively active and the other interferon inducible. *Proc Natl Acad Sci U S A* **96**: 4621–4626. http://dx.doi.org/10.1073/pnas.96.8.4621.

George CX, Wagner MV, Samuel CE. 2005. Expression of interferon-inducible RNA adenosine deaminase ADAR1 during pathogen infection and mouse embryo development involves tissue-selective promoter utilization and alternative splicing. *J Biol Chem* **280**: 15020–15028. http://dx.doi.org/10.1074/jbc.M500476200.

Gorter JA, Petrozzino JJ, Aronica EM, Rosenbaum DM, Opitz T, Bennett MV, Connor JA, Zukin RS. 1997. Global ischemia induces downregulation of Glur2 mRNA and increases AMPA receptor-mediated Ca2+ influx in hippocampal CA1 neurons of gerbil. *J Neurosci* **17**: 6179–6188. http://dx.doi.org/10.1523/JNEUROSCI.17-16-06179.1997.

Hannah MF, Bajic VB, Klein SL. 2008. Sex differences in the recognition of and innate antiviral responses to Seoul virus in Norway rats. *Brain Behav Immun* **22**: 503–516. http://dx.doi.org/10.1016/j.bbi.2007.10.005.

Higuchi M, Maas S, Single FN, Hartner J, Rozov A, Burnashev N, Feldmeyer D, Sprengel R, Seeburg PH. 2000. Point mutation in an AMPA receptor gene rescues lethality in mice deficient in the RNA-editing enzyme ADAR2. *Nature* **406**: 78–81. http://dx.doi.org/10.1038/35017558.

Hur S. 2019. Double-Stranded RNA Sensors and Modulators in Innate Immunity. *Annu Rev Immunol* **37**: 349–375. http://dx.doi.org/10.1146/annurev-immunol-042718-041356.

Jain M, Mann TD, Stulić M, Rao SP, Kirsch A, Pullirsch D, Strobl X, Rath C, Reissig L, Moreth K, et al. 2018. RNA editing of Filamin A pre-mRNA regulates vascular contraction and diastolic blood pressure. *EMBO J* **37**. http://dx.doi.org/10.15252/embj.201694813.

Kawahara Y, Ito K, Sun H, Kanazawa I, Kwak S. 2003. Low editing efficiency of GluR2 mRNA is associated with a low relative abundance of ADAR2 mRNA in white matter of normal human brain. *Eur J Neurosci* **18**: 23–33. http://dx.doi.org/10.1046/j.1460-9568.2003.02718.x.

Klein SL, Flanagan KL. 2016. Sex differences in immune responses. *Nat Rev Immunol* **16**: 626–638. http://dx.doi.org/10.1038/nri.2016.90.

Klein SL, Jedlicka A, Pekosz A. 2010. The Xs and Y of immune responses to viral vaccines. *Lancet Infect Dis* **10**: 338–349. http://dx.doi.org/10.1016/S1473-3099(10)70049-9.

Knutson SD, Arthur RA, Johnston HR, Heemstra JM. 2021. Direct Immunodetection of Global A-to-I RNA Editing Activity with a Chemiluminescent Bioassay. *Angew Chem Int Ed Engl* **60**: 17009–17017. http://dx.doi.org/10.1002/anie.202102762.

Koenig A, Sateriale A, Budd RC, Huber SA, Buskiewicz IA. 2014. The role of sex differences in autophagy in the heart during coxsackievirus B3-induced myocarditis. *J Cardiovasc Transl Res* **7**: 182–191. http://dx.doi.org/10.1007/s12265-013-9525-5.

Li JB, Levanon EY, Yoon J-K, Aach J, Xie B, Leproust E, Zhang K, Gao Y, Church GM. 2009. Genome-wide identification of human RNA editing sites by parallel DNA capturing and sequencing. *Science* **324**: 1210–1213. http://dx.doi.org/10.1126/science.1170995.

Liddicoat BJ, Piskol R, Chalk AM, Ramaswami G, Higuchi M, Hartner JC, Li JB, Seeburg PH, Walkley CR. 2015. RNA editing by ADAR1 prevents MDA5 sensing of endogenous dsRNA as nonself. *Science* **349**: 1115–1120. http://dx.doi.org/10.1126/science.aac7049.

Mannion NM, Greenwood SM, Young R, Cox S, Brindle J, Read D, Nellåker C, Vesely C, Ponting CP, McLaughlin PJ, et al. 2014. The RNA-editing enzyme ADAR1 controls innate immune responses to RNA. *Cell Rep* **9**: 1482–1494. http://dx.doi.org/10.1016/j.celrep.2014.10.041.

Niswender CM, Herrick-Davis K, Dilley GE, Meltzer HY, Overholser JC, Stockmeier CA, Emeson RB, Sanders-Bush E. 2001. RNA editing of the human serotonin 5-HT2C receptor. alterations in suicide and implications for serotonergic pharmacotherapy. *Neuropsychopharmacology* **24**: 478–491. http://dx.doi.org/10.1016/S0893-133X(00)00223-2.

Oh D-B, Kim Y-G, Rich A. 2002. Z-DNA-binding proteins can act as potent effectors of gene expression in vivo. *Proc Natl Acad Sci U S A* **99**: 16666–16671. http://dx.doi.org/10.1073/pnas.262672699.

Patterson JB, Samuel CE. 1995. Expression and regulation by interferon of a double-stranded-RNA-specific adenosine deaminase from human cells: evidence for two forms of the deaminase. *Mol Cell Biol* **15**: 5376–5388. http://dx.doi.org/10.1128/MCB.15.10.5376.

Pestal K, Funk CC, Snyder JM, Price ND, Treuting PM, Stetson DB. 2015. Isoforms of RNA-Editing Enzyme ADAR1 Independently Control Nucleic Acid Sensor MDA5-Driven Autoimmunity and Multi-organ Development. *Immunity* **43**: 933–944. http://dx.doi.org/10.1016/j.immuni.2015.11.001.

Pfaffl MW. 2001. A new mathematical model for relative quantification in real-time RT-PCR. *Nucleic Acids Res* **29**: e45. http://dx.doi.org/10.1093/nar/29.9.e45.

Polson AG, Bass BL. 1994. Preferential selection of adenosines for modification by double-stranded RNA adenosine deaminase. *EMBO J* **13**: 5701–5711. https://www.ncbi.nlm.nih.gov/pubmed/7527340.

Roth SH, Danan-Gotthold M, Ben-Izhak M, Rechavi G, Cohen CJ, Louzoun Y, Levanon EY. 2018. Increased RNA Editing May Provide a Source for Autoantigens in Systemic Lupus Erythematosus. *Cell Rep* **23**: 50–57. http://dx.doi.org/10.1016/j.celrep.2018.03.036.

Saldi T, Riemondy K, Erickson B, Bentley DL. 2021. Alternative RNA structures formed during transcription depend on elongation rate and modify RNA processing. *Mol Cell* **81**: 1789–1801.e5. http://dx.doi.org/10.1016/j.molcel.2021.01.040.

Sans N, Vissel B, Petralia RS, Wang Y-X, Chang K, Royle GA, Wang C-Y, O'Gorman S, Heinemann SF, Wenthold RJ. 2003. Aberrant formation of glutamate receptor complexes in hippocampal neurons of mice lacking the GluR2 AMPA receptor subunit. *J Neurosci* **23**: 9367–9373. http://dx.doi.org/10.1523/JNEUROSCI.23-28-09367.2003.

Schoggins JW. 2019. Interferon-Stimulated Genes: What Do They All Do? *Annu Rev Virol* **6**: 567–584. http://dx.doi.org/10.1146/annurev-virology-092818-015756.

Shallev L, Kopel E, Feiglin A, Leichner GS, Avni D, Sidi Y, Eisenberg E, Barzilai A, Levanon EY, Greenberger S. 2018. Decreased A-to-I RNA editing as a source of keratinocytes' dsRNA in psoriasis. *RNA* **24**: 828–840. http://dx.doi.org/10.1261/rna.064659.117.

Song C, Sakurai M, Shiromoto Y, Nishikura K. 2016. Functions of the RNA Editing Enzyme ADAR1 and Their Relevance to Human Diseases. *Genes* **7**. http://dx.doi.org/10.3390/genes7120129.

Spitzer JA. 1999. Gender differences in some host defense mechanisms. *Lupus* **8**: 380–383. http://dx.doi.org/10.1177/096120339900800510.

Tan MH, Li Q, Shanmugam R, Piskol R, Kohler J, Young AN, Liu KI, Zhang R, Ramaswami G, Ariyoshi K, et al. 2017. Dynamic landscape and regulation of RNA editing in mammals. *Nature* **550**: 249–254. http://dx.doi.org/10.1038/nature24041.

Tariq A, Jantsch MF. 2012. Transcript diversification in the nervous system: a to I RNA editing in CNS function and disease development. *Front Neurosci* **6**: 99. http://dx.doi.org/10.3389/fnins.2012.00099.

Tossberg JT, Heinrich RM, Farley VM, Crooke PS 3rd, Aune TM. 2020. Adenosine-to-Inosine RNA Editing of Alu Double-Stranded (ds)RNAs Is Markedly Decreased in Multiple Sclerosis and Unedited Alu dsRNAs Are Potent Activators of Proinflammatory Transcriptional Responses. *J Immunol* **205**: 2606–2617. http://dx.doi.org/10.4049/jimmunol.2000384.

Wang IX, So E, Devlin JL, Zhao Y, Wu M, Cheung VG. 2013. ADAR regulates RNA editing, transcript stability, and gene expression. *Cell Rep* **5**: 849–860. http://dx.doi.org/10.1016/j.celrep.2013.10.002.

Wang Q, O'Brien PJ, Chen CX, Cho DS, Murray JM, Nishikura K. 2000. Altered G protein-coupling functions of RNA editing isoform and splicing variant serotonin2C receptors. *J Neurochem* **74**: 1290–1300. http://dx.doi.org/10.1046/j.1471-4159.2000.741290.x.

Weinstein Y, Ran S, Segal S. 1984. Sex-associated differences in the regulation of immune responses controlled by the MHC of the mouse. *J Immunol* **132**: 656–661. https://www.ncbi.nlm.nih.gov/pubmed/6228595.

Werry TD, Loiacono R, Sexton PM, Christopoulos A. 2008. RNA editing of the serotonin 5HT2C receptor and its effects on cell signalling, pharmacology and brain function. *Pharmacol Ther* **119**: 7–23. http://dx.doi.org/10.1016/j.pharmthera.2008.03.012.

Wong SK, Sato S, Lazinski DW. 2001. Substrate recognition by ADAR1 and ADAR2. *RNA* **7**: 846–858. http://dx.doi.org/10.1017/s135583820101007x.

Yu Z, Chen T, Cao X. 2015. RNA editing by ADAR1 marks dsRNA as "self." *Cell Res* **25**: 1283–1284. http://dx.doi.org/10.1038/cr.2015.135.

APPENDICES

Appendix A. Missouri State University IBC Approval

Missouri State UNIVERSITY

MEMORANDUM OF UNDERSTANDING & AGREEMENT (MUA) FOR RECOMBINANT DNA EXPERIMENTS

All MUA'S can be submitted electronically to researchadministration@missouristate.edu or submitted as a hard copy to the ORA in Carrington 405. A signed copy must be provided. The *NIH Guidelines for Research Involving Recombinant DNA Molecules* should be used as a reference when completing this MUA (see http://oba.od.nih.gov/rdna/nih_guidelines_oba.html).

A. General Information

Date: 4-8-2022

Researcher Name: Dr. Randi Ulbricht

Researcher Title: Assistant Professor

Phone: 836-5730

Department: Biomedical Science

Office Bldg & Room #:   PROF 343

Laboratory Bldg & Room #:   PROF 340 and PROF 360

Granting Agency:

Grant Number (if applicable):

Title of Grant or Project: RNA editing

B. Project Information

1. **Describe the experiments involving recombinant DNA techniques. Your description is to be sufficiently complete so as to provide committee members an understanding of what you intend to do and how you will do it. A summary or abstract of your methods and materials section may also be provided if needed for clarity.**

My laboratory will be performing basic cloning techniques to generate plasmid DNA constructs for transfection of bacteria and mammalian cell culture. We will perform restriction enzyme digestion and ligation reactions *in vitro*, transform the ligated products into *E. coli* laboratory strains (i.e. DH5α or DH10β) for propagation, isolate and purify the recombinant DNA from *E. coli* lysates, and finally, transfect mammalian cells for eventual isolation and analysis of RNA editing levels in the mammalian cells. We will also utilize small synthetic nucleic acid polymers for PCR-based cloning applications and diagnostic purposes.

The genes and gene fragments involved in these cloning procedures are related to RNA editing (editing enzymes and substrates) and are not pathogenic in nature. The plasmid backbones are commercially available and contain antibiotic resistance markers (i.e. Ampicillin and Kanamycin).

2. **Provide an assessment of the physical containment required for the experiments.**

All procedures will be performed in laboratory space (PROF340 or PROF360) or utilizing other necessary equipment (i.e. incubators, centrifuges, ect) also on the 3rd floor of Professional Building. Non-absorptive working surfaces are lined with absorptive bench paper that has a plastic backing for containment of spills.

3. Describe the facilities and specific procedures which will be used to provide the required levels of containment.

The laboratory space contains a door that locks. The space will be cleaned with disinfectant prior to and after performing laboratory procedures. Disinfectants used include simple green and 70% ethanol. All personnel will be trained on proper laboratory techniques on the safe handling of recombinant DNA.

4. Describe the procedures and precautions to be followed if biohazardous organisms or agents are to be transported between laboratories.

If reagents (DNA) or organisms (*E. coli* or mammalian cells) are to be transferred, they will be transported in primary and secondary containment vessels. Both vessels will be made of plastic, whenever possible. (It is possible that the primary vessel will be glass culture tubes.) A layer of absorptive paper towel will be placed between the primary and secondary containers to help contain any spills.

5. Describe the waste disposal procedures expected to be used during this experiment.

All waste generated in these procedures will be autoclaved or treated with 10% bleach solution for >30min prior to disposal. Autoclaves are located in PROF 360 or PROF 372.

6. Will this project involve environmental release? If yes, please provide a description of the release.

This project will NOT involve environmental release.

7. Please list all students, staff and faculty involved with this project. CITI Biosafety training is mandatory for all personnel working with biohazards prior to final IBC approval.

Randi Ulbricht
Christian Rivas
Anna McWoods

59

8. **The undersigned agree to certify the following conditions of the proposed research:**

   a. The information above is accurate and complete.
   b. We agree to accept responsibility for training of all laboratory workers involved in the project.
   c. We agree to comply with all appropriate requirements pertaining to shipment and of hazardous biological and recombinant DNA materials.
   d. We are familiar with and agree to abide the provisions of the Missouri State University policies and procedures applicable to experiments involving recombinant DNA, the provisions of the current *NIH Guidelines for Research Involving Recombinant DNA Molecules,* and any other specific instructions pertaining to the proposed project.

	4-8-2022		
Principal Investigator	Date	Department Head	Date

9. **The Institutional Biosafety Committee has determined, based on information provided the principal investigator, that:**

   a. No special medical surveillance (other than usual University health programs) is required for the project described in this MUA
   b. The following specific medical surveillance procedures must be carried out, for individuals listed by name, before commencing the project described in this MUA:

10. **We certify that the Missouri State University Institutional Biosafety Committee has reviewed the proposed project for recombinant DNA experiments for compliance with the current *NIH Guidelines for Research Involving Recombinant DNA Molecules* and Missouri State University's policies and procedures applicable to experiments involving recombinant DNA. The MSU IBC will monitor throughout the duration of the project the facilities, procedures, and the training and expertise of the personnel involved in the recombinant DNA activity.**

MSU IBC Chair or Representative	Date

Appendix B. CITI Certification

CITI PROGRAM

Completion Date 23-Mar-2023
Expiration Date 23-Mar-2025
Record ID 51164828

This is to certify that:

Kelsey Kendrick

Has completed the following CITI Program course:

Biosafety and Biosecurity (BSS)
(Curriculum Group)
Basic Biosafety Course
(Course Learner Group)
1 - Basic Course
(Stage)

Under requirements set by:

Missouri State University

Not valid for renewal of
certification through CME.

CITI
Collaborative Institutional Training Initiative

101 NE 3rd Avenue, Suite 320
Fort Lauderdale, FL 33301 US
www.citiprogram.org